Supporting Information

Self-assembly of azaphthalocyanine-oligodeoxynucleotide conjugates into J-dimers: towards biomolecular logic gates

Jiri Demuth,[a] Miroslav Miletin,[a] Radim Kucera,[a] Ales Ruzicka,[b] Zuzana Havlinova,[ac] Antonin Libra,[c] Veronika Novakova,[a] Petr Zimcik*,[a]

[a] Department of Pharmaceutical Chemistry and Pharmaceutical Analysis, Charles University, Faculty of Pharmacy in Hradec Králové, Akademika Heyrovského 1203/8, 500 05 Hradec Kralove, Czech Republic, zimcik@faf.cuni.cz

[b] Department of General and Inorganic Chemistry, Faculty of Chemical Technology, University of Pardubice, Studentská 573, 532 10, Pardubice, Czech Republic

[c] Generi Biotech, Machkova 587, Hradec Kralove, 500 11, Czech Republic

Content:

Synthesis

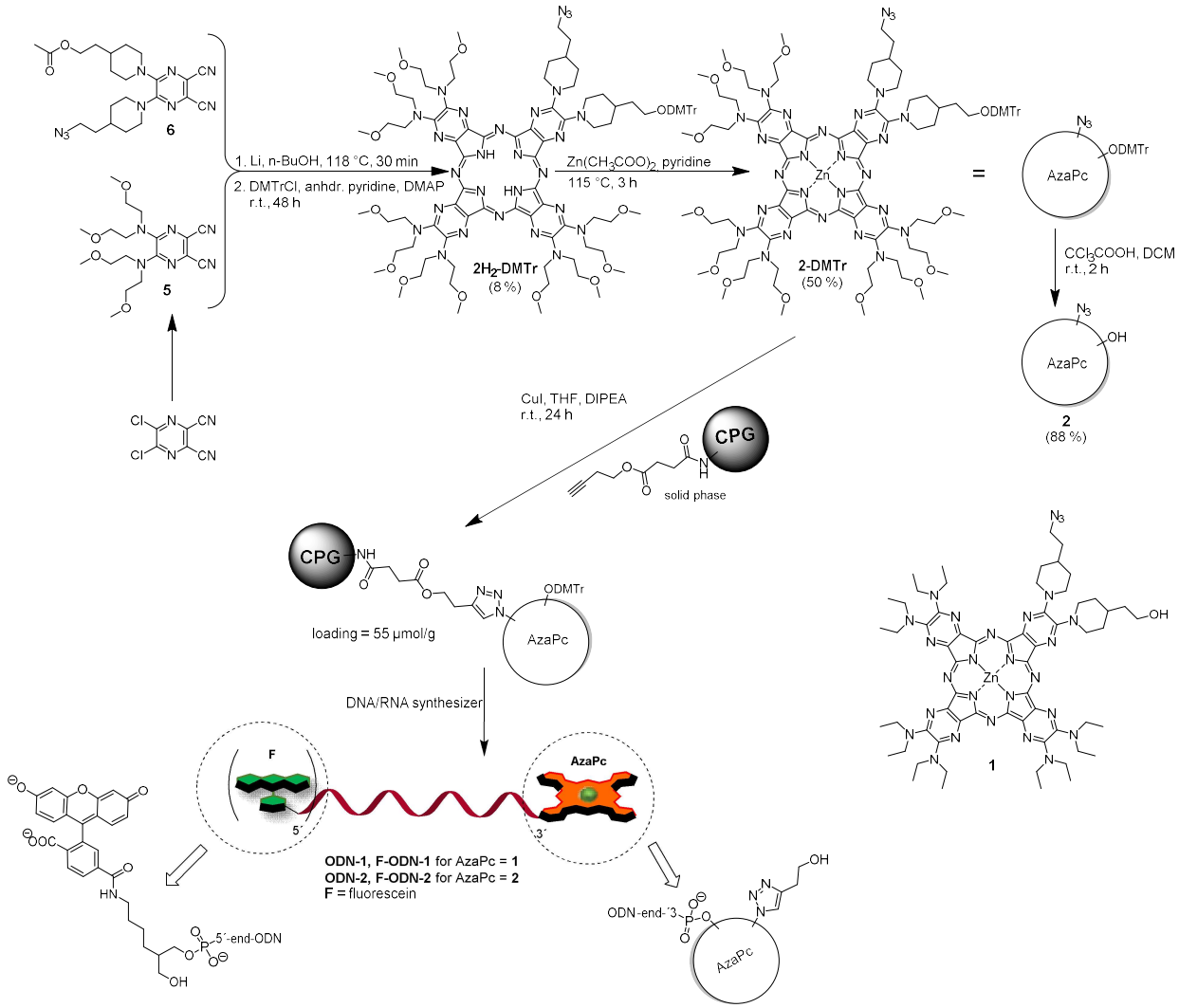

Scheme S1. Synthesis of the investigated compounds and ODN probes.

Precursors for AzaPcs, *i.e.* disubstituted pyrazine-2,3-dicarbonitriles, were prepared by nucleophilic substitution starting from 5,-6-dichloro-pyrazine-2,3-dicarbonitrile. Thus, reaction with bis(2-methoxy)ethylamine provided 5,6-bis[bis(2-methoxyethyl)amino]pyrazine-2,3-dicarbonitrile (**5**) in 99 % yield. Precursor **6** bearing hydroxy and azido groups was synthesized in four steps similarly as published before.[1]

Synthesis of AzaPc **2** and **4** followed the protocol recently developed for AzaPcs **1** and **3** (Scheme S1).[1] Briefly, lithium butoxide-induced mixed cyclotetramerization of precursor **5** and **6** yielded mixture of six congeners of the metal-free AzaPc. The retention factors of all congeners were, however, very close each other. For this reason, the desired congener **$2H_2$-DMTr** (8 % yield) was isolated after reaction of the whole mixture with dimethoxytritylchloride (DMTrCl) that protected the OH groups and made the individual congeners easily separable. Coordination of central zinc (II) cation using zinc acetate in

pyridine was achieved in 50 % yield leading to **2-DMTr** that was deprotected to **2** (88 %). Direct cyclotetramerization of **5** yielded 60 % of metal-free ligand that was converted to **4** in 64 %.

Similarly to synthesis of the ODN probes bearing AzaPc **1**,[1] AzaPc **2-DMTr** was subsequently attached to controlled-pore glass solid phase (achieved loading 55 µmol/g, based on the released DMTr) and introduced into DNA/RNA synthesizer. The selected ODNs (Chart 2) were then synthesized and eventually modified by fluorescein on 5' -end if requested. The probes were then cleaved from the solid phase, purified by HPLC and characterized by MALDI spectra (Fig. S1). Unmodified antisense **ODN-ant** (Chart 2) with part of its sequence complementary to complete sequence of the labeled probes was used in some experiments.

General

All organic solvents used in the synthesis were of analytical grade. Anhydrous butanol used for the cyclotetramerization was freshly distilled from magnesium. All other chemicals for the syntheses were purchased from certified suppliers (i.e. TCI Europe, Acros, and Merck) and used as received. TLC was performed on Merck aluminium sheets coated with silica gel 60 F254. Merck Kieselgel 60 (0.040–0.063 mm) was used for column chromatography. The ^{1}H and ^{13}C NMR spectra were recorded on a Varian VNMR S500 NMR spectrometer. The chemical shifts are reported as δ values in ppm and are indirectly referenced to $Si(CH_3)_4$ *via* the signal from the solvent. *J* values are given in Hz. The UV/Vis spectra were recorded using a Shimadzu UV-2600 spectrophotometer. The fluorescence spectra were measured using an FS5 Spectrofluorometer (Edinburg Instruments). HRMS spectra were measured at UHPLC system Acquity UPLC I-class (Waters, Millford, USA) coupled to high resolution mass spectrometer (HRMS) Synapt G2Si (Waters, Manchester, UK) based on Q-TOF were used for HRMS spectra measurement. Chromatography was carried out using Acquity UPLC Protein BEH C4 (2.1 x 50mm, 1.7 µm, 300 Å) column using gradient elution with ACN and 0.1% formic acid at flow-rate 0.4 ml/min. Electrospray ionization was operated in positive ion mode. The ESI spectra were recorded in the range 50 - 5000 m/z using leucine-enkefaline as a lock mass reference and sodium iodide for external calibration or in the range 50 - 1200 m/z using leucine-enkefaline as a lock mass reference and sodium formate for external calibration. Mass spectra of the oligonucleotide probes were obtained using a MALDI-TOF Bruker Autoflex II mass spectrometer with 3-hydroxypicolinic acid and ammonium citrate in 50% acetonitrile as a matrix.

Synthesis of AzaPcs

AzaPc **1**,[1] AzaPc **3**,[2] and 2-(1-{3-[4-(2-azidoethyl)piperidin-1-yl]-5,6-dicyanopyrazin-2-yl}piperidin-4-yl)ethyl acetate (**6**)[1] were prepared according to the published procedures.

***5,6-bis[bis(2-methoxyethyl)amino]pyrazine-2,3-dicarbonitrile* (5):**

5,6-dichloropyrazine-2,3-dicarbonitrile (3.00 g, 15.00 mmol) was dissolved in THF (100 mL). Bis(2-methoxy)ethylamine (13.26 mL, 90.00 mmol) was added dropwise at rt. After that, reaction was heated at 70°C for 5 hours. The solvent was then evaporated and the solid residue was dissolved in ethyl acetate (80 mL), and washed with water (3×100 mL). The layers were separated each other; remaining product was extracted from water with ethyl acetate (2×100 mL). Organic layers were collected, dried over anhydrous Na_2SO_4 and solvent was evaporated to dryness. Crude product was purified by column chromatography on silica with ethyl acetate/acetone 10:1 (R_f=0.6) as an eluent and recrystallized from methanol. Yield: 5.85 g (99%) as orange-yellow crystals. M.p. 71.0-71.2 °C. ^{1}H NMR (500 MHz, Acetone-d_6) δ 3.81 (t, *J* = 5.1 Hz, 8H), 3.47 (t, *J* = 5.1 Hz, 8H), 3.18 (s, 12H) ppm. ^{13}C NMR (126 MHz, Acetone-d_6) δ 148.23, 120.31, 116.12, 70.52, 58.62, 49.26 ppm. HRMS (ESI) (m/z): calculated for $[M+H]^+$ ($C_{18}H_{29}N_6O_4^+$) requires 393.2245, found 393.2249.

***2-[4-(2-azidoethyl)piperidin-1-yl]-3-[4-(2-dimethoxytrityloxyethyl)-piperidin-1-yl]-9,10,16,17,23,24-hexakis[bis(2-methoxyethyl)amino]-1,4,8,11,15,18,22,25-octaazaphthalocyanine* ($2H_2$-DMTr):**

Compounds **6** (1.0 g, 2.22 mmol) and **5** (2.61 g, 6.66 mmol) were dissolved in anhydrous butanol, heated to reflux and metal lithium was added (460 mg, 66.6 mmol). Reaction mixture was heated at reflux for 30 minutes. Butanol was evaporated under reduce pressure and a mixture of DCM/2% HCl 1:1 (150 mL) was added. Product was extracted by DCM (3×50 mL). Organic layers were collected and evaporated to dryness under reduced pressure by azeotropic distillation with toluene. According to TLC, the congeners in the mixture had similar R_f disabling isolation of desired congener. Therefore, the mixture of congeners was only pre-purified by column chromatography on silica with DCM/MeOH 12:1 as an eluent (fractions with R_f around 0.47 containing mostly desired congener were collected).

Free hydroxy groups on AzaPc periphery resulting from a spontaneous deprotection of precursor **6** by lithium butoxide used for cyclotetramerization were modified by the following procedure: Pre-purified congener (1.67 g, approx. 1 mmol) and 4,4'-dimethoxytrityl chloride (4.31 g, 12.72 mmol) were dissolved in an anhydrous pyridine (15 mL) under inert atmosphere and few crystals of 4-dimethylaminopyridine were added. Reaction mixture was stirred at rt for 48 hours. Reaction mixture was evaporated to dryness. Product was purified by column chromatography on silica with DCM/THF/MeOH 40:1:1 (R_f=0.43) as an eluent. Finally, the product was dissolved in a minimal amount of DCM (approx. 0.5 mL), dropped into hexane (100 mL) and stored at a freezer at −18 °C overnight.

Precipitate was collected and thoroughly dried. Yield: 320 mg (8 %) of purple crystals. M.p. > 300°C. ^{1}H NMR (500 MHz, Pyridine-d_5) δ 7.87 – 7.81 (m, 2H), 7.73 – 7.66 (m, 4H), 7.54 – 7.49 (m, 2H), 7.40 – 7.35 (m, 1H), 7.15 – 7.08 (m, 4H), 4.81 – 4.70 (m, 4H), 4.45 – 4.39 (m, 16H), 4.39 – 4.34 (m, 8H), 3.77 (s, 6H), 3.77 – 3.72 (m, 16H), 3.72 – 3.66 (m, 8H), 3.47 – 3.41 (m, 2H), 3.35 (t, *J* = 7.1 Hz, 2H), 3.24 (s, 18H), 3.23 (s, 6H), 3.22 (s, 6H), 3.21 (s, 6H), 3.11 – 3.03 (m, 4H), 1.98 – 1.78 (m, 8H), 1.59 – 1.43 (m, 6H), -1.49 (s, 2H) ppm. ^{13}C NMR (126 MHz, Pyridine-d_5) δ 158.9, 150.9, 150.8, 150.6, 149.5, 137.1, 135.3, 135.1, 130.5, 128.6, 128.1, 127.0, 123.3, 123.1, 113.5, 71.0, 70.9, 70.9, 61.3, 58.3, 58.3, 55.1, 49.0, 48.9, 48.8, 48.8, 47.8, 47.5, 36.9, 35.2, 33.7, 33.5, 32.6, 32.1 ppm (some aromatic signals fused together). HRMS (ESI) (m/z): calculated for $[M+H]^+$ ($C_{95}H_{132}N_{27}O_{15}^+$) requires 1891.0391, found 1891.0325.

2-[4-(2-azidoethyl)piperidin-1-yl]-3-[4-(2-dimethoxytrityloxyethyl)-piperidin-1-yl]-9,10,16,17,23,24-hexakis[bis(2-methoxyethyl)amino]-1,4,8,11,15,18,22,25-octaazaphthalocyaninato zinc(II) **(2-DMTr):**

Metal-free **$2H_2$-DMTr** (290 mg, 0.15 mmol) was dissolved in anhydrous pyridine (5 mL) and zinc (II) acetate (169 mg, 0.96 mmol) was added. Reaction was stirred and refluxed for 3 hours. Pyridine was removed under reduced pressure and product was purified by column chromatography on silica with DCM/MeOH 22:1 (R_f=0.37) as an eluent. Finally, the product was dissolved in a minimal amount of DCM (approx. 0.5 mL), dropped into hexane (100 mL) and stored at a freezer at −18 °C overnight. Precipitate was collected and thoroughly dried. Yield:150 mg (50 %) of dark blue crystals. M.p. > 300°C. ^{1}H NMR (500 MHz, Pyridine-d_5) δ 7.86 – 7.81 (m, 2H), 7.71 – 7.67 (m, 4H), 7.52 (t, *J* = 7.8 Hz, 2H), 7.40 – 7.35 (m, 1H), 7.14 – 7.09 (m, 4H), 4.81 – 4.70 (m, 4H), 4.45 – 4.40 (m, 16H), 4.40 – 4.35 (m, 8H), 3.78 (s, 6H), 3.77 – 3.73 (m, 16H), 3.72 – 3.67 (m, 8H), 3.44 (t, *J* = 6.4 Hz, 2H), 3.37 – 3.32 (m, 2H), 3.23 (d, *J* = 1.3 Hz, 24H), 3.21 (s, 6H), 3.20 (s, 6H), 3.14 – 3.03 (m, 4H), 1.97 – 1.78 (m, 8H), 1.59 – 1.42 (m, 6H) ppm. ^{13}C NMR (126 MHz, Pyridine-d_5) δ 159.1, 151.5, 149.6, 142.8, 137.3, 135.5, 135.3, 130.7, 128.8, 128.3, 123.5, 123.3, 113.7, 71.2, 71.2, 71.1, 58.5, 58.4, 55.3, 49.2, 49.2, 49.1, 49.0, 48.0, 47.7, 35.4, 32.8, 32.3 ppm (some aromatic signals fused together). HRMS (ESI) (m/z): calculated for $[M+H]^+$ ($C_{95}H_{130}N_{27}O_{15}Zn^+$) requires 1952.9526, found 1952.9515.

2-[4-(2-azidoethyl)piperidin-1-yl]-3-[4-(2-hydroxyethyl)-piperidin-1-yl]-9,10,16,17,23,24-hexakis[bis(2-methoxyethyl)amino]-1,4,8,11,15,18,22,25-octaazaphthalocyaninato zinc(II) **(2):**

Trichloroacetic acid (5.4 µL, 0.05 mmol) was added to **2-DMTr** (50 mg, 0.03 mmol) dissolved in DCM (5 mL) and the reaction mixture was stirred for 2 hours at rt. After that, DCM (30 mL) was added and product was washed with 5% $NaHCO_3$ (3×20 mL). Organic phase was dried over anhydrous Na_2SO_4 and evaporated to dryness. Crude product was purified by column chromatography on silica with DCM/MeOH (15:1) as an eluent (R_f=0.31). Yield: 37 mg (88 %) of dark blue crystals. M.p. > 300°C. ^{1}H

NMR (500 MHz, Pyridine-d_5) δ 4.78 (t, *J* = 9.4 Hz, 4H), 4.44 – 4.38 (m, 16H), 4.38 – 4.33 (m, 8H), 4.04 (t, *J* = 6.5 Hz, 2H), 3.77 – 3.71 (m, 16H), 3.71 – 3.65 (m, 8H), 3.34 (t, *J* = 7.1 Hz, 2H), 3.23 (s, 24H), 3.20 (s, 6H), 3.20 (s, 6H), 3.16 – 3.02 (m, 4H), 2.09 – 2.03 (m, 2H), 1.99 (br, 1H), 1.91 – 1.80 (m, 4H), 1.73 – 1.41 (m, 8H) ppm. ^{13}C NMR (126 MHz, Pyridine-d_5) δ 151.53, 151.44, 151.30, 150.91, 149.66, 143.22, 143.10, 142.88, 142.84, 135.51, 135.31, 123.50, 123.30, 71.22, 71.13, 59.72, 58.47, 49.20, 49.12, 49.02, 48.07, 47.76, 40.47, 35.41, 33.94, 33.47, 33.00, 32.33 ppm (some aromatic signals fused together). UV/Vis (THF): λ_{max} (log ε) = 654 (5.4), 596 (4.6), 505 (4.6), 373 nm (5.2). HRMS (ESI) (m/z): calculated for $[M+H]^+$ ($C_{74}H_{112}N_{27}O_{13}Zn^+$) requires 1650.8219, found 1650.8181.

2, 3, 9, 10, 16, 17, 23, 24-octakis[bis(2-methoxyethyl)amino]-1,4,8,11,15,18,22,25-octaazaphthalocyane (4H₂):

Compound **4** (300 mg, 0.76 mmol) was dissolved in anhydrous BuOH (5 mL), heated to reflux and lithium (38 mg, 5.42 mmol) was added. Reaction mixture was heated at 118 °C for 1 hour. Butanol was evaporated under vacuum. Solid residue was dissolved in mixture of DCM/2% HCl 1:1 (40 mL), product was than extracted with DCM (3×20 mL). Organic layers were collected and evaporated under reduced pressure by azeotropic distillation with toluene. Product was purified by column chromatography on silica with DCM/MeOH (15:1) as eluent (R_f=0.22). Finally, the product was dissolved in a minimal amount of DCM (approx. 0.5 mL), dropped into hexane (100 mL) and stored at a freezer at −18 °C overnight. Precipitate was collected and thoroughly dried. Yield: 180 mg (60 %) of dark purple crystals. M.p. > 300°C. ^{1}H NMR (500 MHz, Pyridine-d_5) δ 4.39 (t, *J* = 5.4 Hz, 32H), 3.73 (t, *J* = 5.3 Hz, 32H), 3.21 (d, *J* = 1.3 Hz, 48H), -1.56 (s, 2H) ppm. ^{13}C NMR (126 MHz, Pyridine-d_5) δ 150.84, 141.16, 71.13, 58.49, 49.11 ppm (one aromatic signal is overlapped by solvent signal). HRMS (ESI) (m/z): calculated for $[M+H]^+$ ($C_{72}H_{115}N_{24}O_{16}^+$) requires 1571.8917, found 1571.8879

2, 3, 9, 10, 16, 17, 23, 24-octakis[bis(2-methoxyethyl)amino]-1,4,8,11,15,18,22,25-octaazaphthalocyaninato zinc(II) (4):

Compound **4H₂** (700 mg, 0.45 mmol) was dissolved in pyridine (15 mL) and zinc (II) acetate (490 mg, 2.67 mmol) was added. Reaction mixture was heated at 115 °C for 3 hours, followed by evaporation of pyridine. Product was obtained by column chromatography on silica with DCM/MeOH (15:1) as a mobile phase (R_f=0.58). Finally, the product was dissolved in a minimal amount of DCM (approx. 0.5 mL), dropped into hexane (100 mL) and stored at a freezer at −18 °C overnight. Precipitate was collected and thoroughly dried. Yield: 467 mg (64 %) as dark blue crystals. M.p. > 300°C. ^{1}H NMR (500 MHz, Pyridine-d_5) δ 4.39 (t, *J* = 5.5 Hz, 32H), 3.72 (t, *J* = 5.5 Hz, 32H), 3.22 (d, *J* = 0.7 Hz, 48H) ppm. ^{13}C NMR (126 MHz, Pyridine-d_5) δ 151.21, 142.82, 71.20, 58.46, 49.12 ppm (one aromatic signal is

overlapped by solvent signal). UV/Vis (THF): λ_{max} (log ε) = 666 (5.3), 599 (4.5), 508 (4.6), 374 nm (5.1). HRMS (ESI) (m/z): calculated for $[M+H]^+$ ($C_{72}H_{113}N_{24}O_{16}Zn^+$) requires 1633.8052, found 1633.7996

Synthesis, purification and characterization of ODN probes

Solid phase modified with AzaPc

AzaPc **2-DMTr** (24 mg, 0.012 mmol) and CuI (34 mg, 0.180 mmol) were dissolved in THF/diisopropylethylamine (2:1 v/v, 1 mL) and added to the alkyne-modified solid phase (120 mg) prepared according to the literature.[3] The suspension was shaken at rt for 24 h. Then, solvent in the vial with the solid phase was removed by decantation, solid phase was washed successively with THF, acetonitrile, dichloromethane, and diethyl ether (4×1 mL of each) and dried under vacuum over the P_2O_5. The loading of AzaPc to the solid phase was determined using absorption spectroscopy and monitoring the band corresponding to 4,4'-dimethoxytrityl (*i.e.*, at 498 nm) released from the solid phase. The procedure was as follows: approximately 2–3 mg of the support was accurately weighed directly to the test tube, perchloric acid solution (10 mL, 70% $HClO_4$/methanol in ratio 52:46) was then added, the test tube was sealed and shaken for 30 min. The sample was diluted, transferred to 1 cm cuvette and absorbance at 498 nm was measured. The loading was calculated as follows:

$$loading\ (\mu mol/g) = \frac{A_{498\,nm} \times dilution \times 143}{weight\ of\ support\ in\ mg}$$

The loading of the solid phase by AzaPc **2-DMTr** was 55 µmol/g.

ODNs labeled with AzaPc

ODNs (**ODN-1**, **ODN-2**, **F-ODN-2**) were synthesized with a Perkin– Elmer Applied Biosystems 394 DNA/RNA synthesizer using the modified solid phase by the Generi Biotech company (Hradec Kralove, Czech Republic). Synthesis and characterization of **F-ODN-1** was published before.[1] For **F-ODN-2**, the 5'-labeling by fluorescein was performed on the same synthesizer employing standard phosphoramidite chemistry and 6-Fluorescein Phosphoramidite (Glen Research, Sterling, VA, USA, Catalog No 10-1964). All labeled ODNs were synthesized using standard protected phosphoramidite monomers and were cleaved from the solid support and deprotected by treatment with 32% ammonia solution at rt for 24 h. After that, the crude oligonucleotides were passed through a hydrated gel filtration column (CentriPure N10, empBIOTECH, Germany) in order to remove the low molecular weight impurities. The blue/purple fractions (eluted with water) were quantified by absorbance at 260 nm, then evaporated to dryness under high vacuum (4 mbar) and dissolved in water to the approximate concentration of 1 mM for HPLC purification. Chromatographic conditions: The purity of **ODN-1, ODN-2** and **F-ODN-2** after semi-preparative purification was assessed by HPLC. The separation was performed on a Hypersil BDS C18 column (100 × 4.6 mm, particle size 2.4 μm) using a mobile phase

consisting of acetonitrile-TEAA (5 mM, pH 6.3), 34:66, v/v (**ODN-1**) and 25:75, v/v (**ODN-2, F-ODN-2**). The column temperature was maintained at 40 °C, and the flow rate was set at 1.0 mL/min. The compounds were analysed by a diode array detector and the chromatograms were monitored at 650 nm. The chromatograms and three-point purity of principal compound was assessed as the purity criterion. The semi-preparative purification was accomplished under the same conditions, but the amount of acetonitrile in the mobile phase was decreased by 1%. After the purification, the desired ODNs were obtained by freeze-drying as purple-black solid. Purified oligonucleotides were stored at -20 °C.

ODN-1: MS (MALDI-TOF): clusters peaking at *m/z* 8801 $[M+H]^+$ and 4401 $[M+2H]^{2+}$. UV/Vis (hybridization buffer): λ_{max} (log ε) = 680 (4.6), 540 (4.6), 377 (5.0), 259 nm (5.4). HPLC: t_R = 13.2 min.

ODN-2: MS (MALDI-TOF): clusters peaking at *m/z* 9163 $[M+H]^+$ and 4582 $[M+2H]^{2+}$. UV/Vis (hybridization buffer): λ_{max} (log ε) = 664 (5.1), 535 (4.5), 376 (5.0), 258 nm (5.3). HPLC: t_R = 10.8 min.

F-ODN-2: MS (MALDI-TOF): clusters peaking at *m/z* 9701 $[M+H]^+$ and 4851 $[M+2H]^{2+}$. UV/Vis (hybridization buffer): λ_{max} (log ε) = 669 (5.2), 609 (4.5), 494 (4.7), 381 (5.2), 257 nm (5.4). HPLC: t_R = 12.3 min.

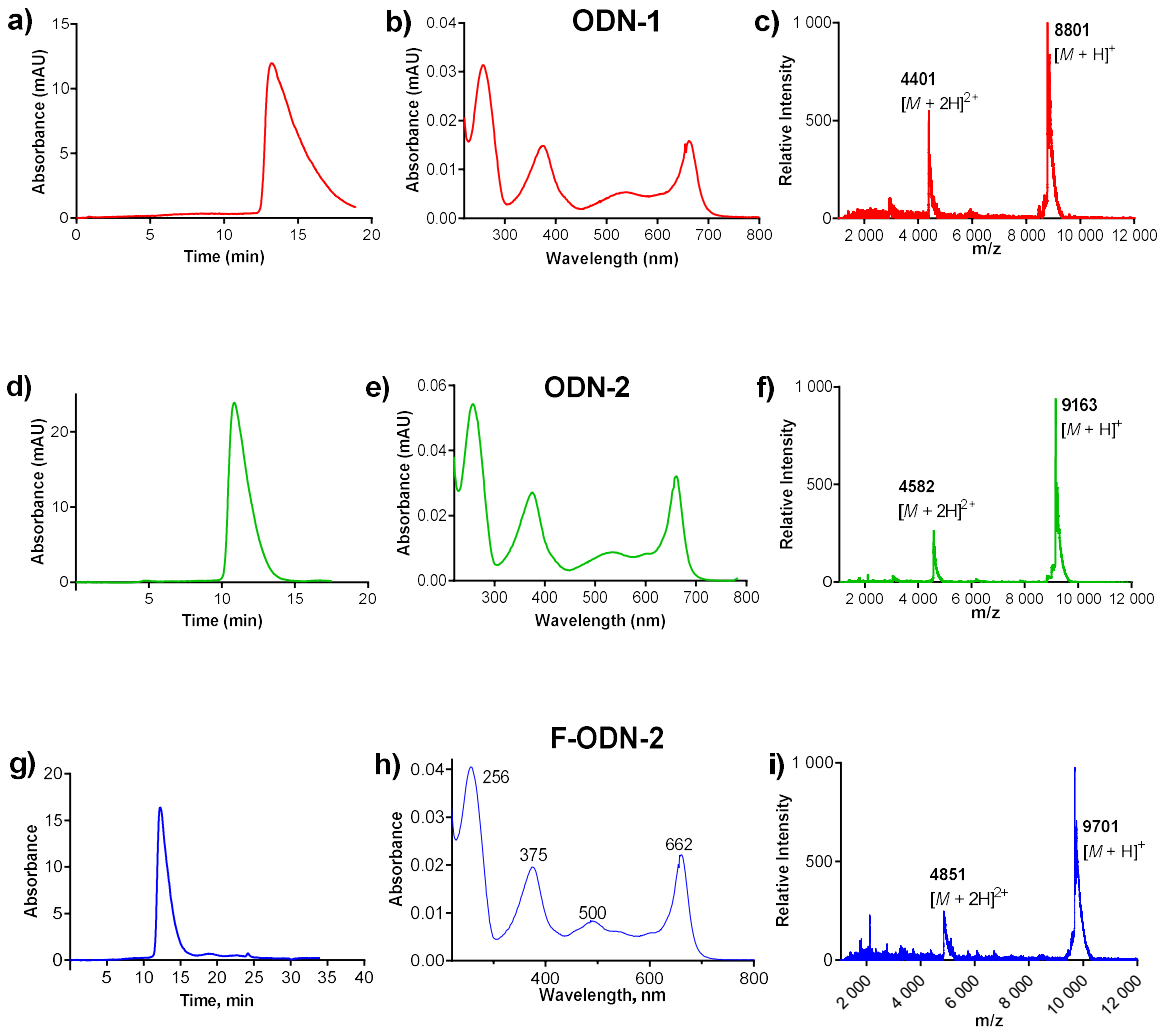

Fig. S1. a, d, g) HPLC chromatogram of **ODN-1** (a) (λ = 650 nm, three-point purity—similarity 0. 9999), **ODN-2** (d) (λ = 650 nm, three-point purity—similarity 0. 9999), and **F-ODN-2** (g) (λ = 650 nm, three-point purity—similarity 0. 9999). b, e, h) absorption spectrum from HPLC peak for **ODN-1** (b, at t = 13.2 min), **ODN-2** (e, at t = 10.8 min), and **F-ODN-2** (h, at t = 12.3 min). Spectra contain typical features of a ODN chain (256 nm), AzaPc (~375 and ~662 nm) and fluorescein (500 nm, only in **F-ODN-2**). c, f, i) MALDI mass spectrum of **ODN-1** (c), **ODN-2** (f) and **F-ODN-2** (i). HPLC conditions: Hypersil BDS C18 column (100 × 4.6 mm, particle size 2.4 μm), mobile phase acetonitrile-TEAA (5 mM, pH 6.3), 34:66, v/v (**ODN-1**) and 25:75, v/v (**ODN-2, F-ODN-2**).

Crystallography - figures

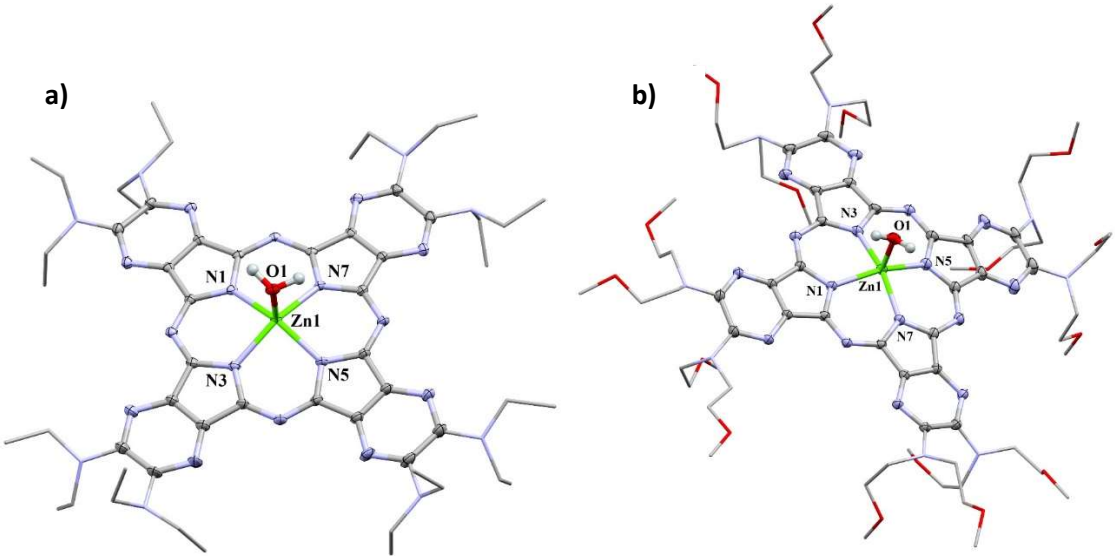

Fig. S2. The molecular structure of single molecule of **3** (a) and **4** (b). Color codes: nitrogen – blue, zinc – green, oxygen – red, carbon – grey, hydrogen – white.

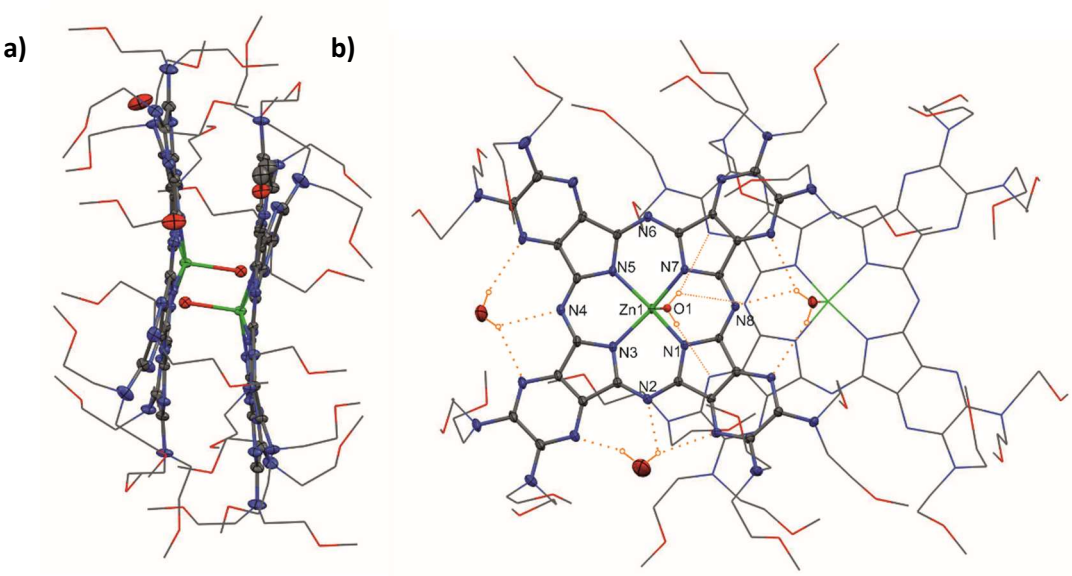

Fig. S3: A dimeric arrangement of molecule **4** in crystalline material. Side (a) and top (b) view. Color codes: nitrogen – blue, zinc – green, oxygen – red, carbon – grey, water hydrogens – orange. For the sake of clarity, other hydrogens are not shown. H-bridges in the dimeric arrangement are highlighted in orange.

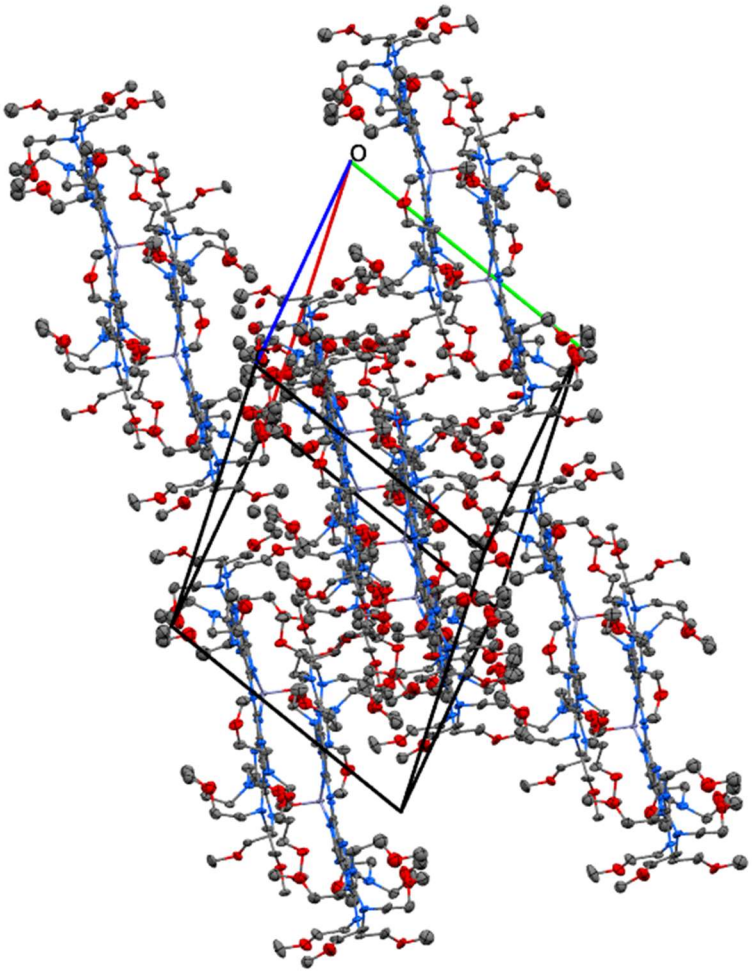

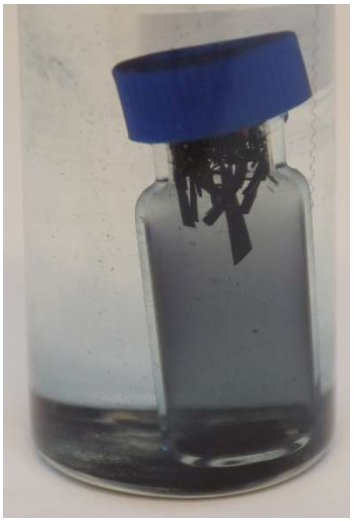

Fig. S4: Supramolecular architecture of layered structure of **4** and the picture of grown crystals.

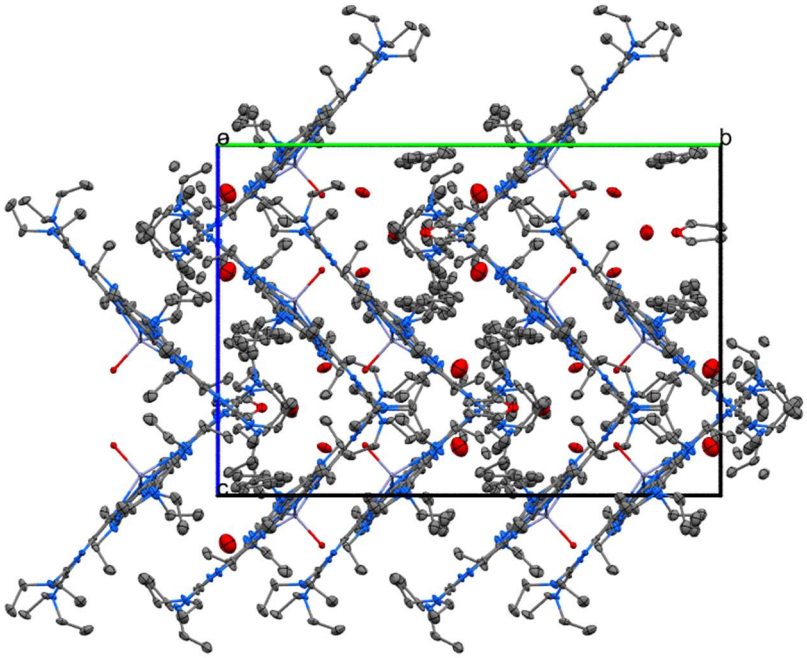

Fig. S5: Supramolecular architecture of layered structure of **3**.

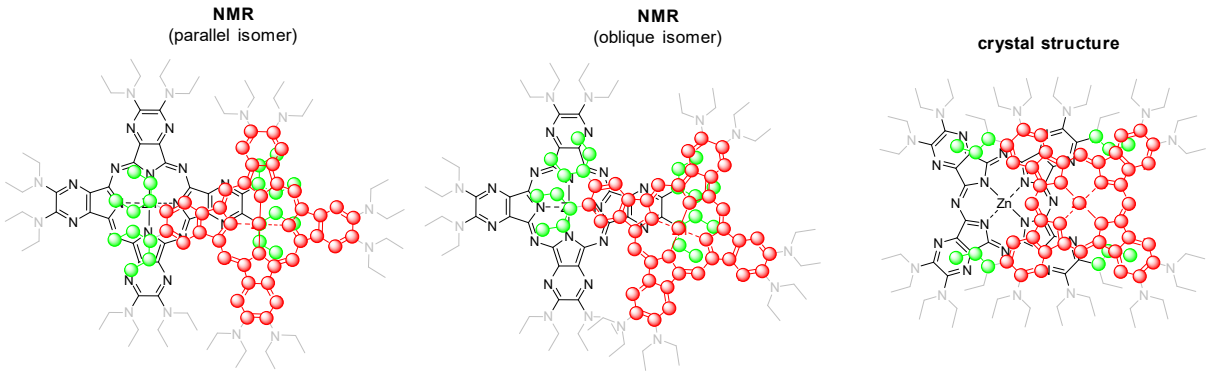

Fig S6. Schematic illustration of the J-dimers **(3)$_2$** viewed from the top. In toluene solution, NMR confirmed formation of J-dimers (two isomers are possible (parallel and oblique)) formed by coordination of central zinc (II) with nitrogen of diethylamino substituent. XRD of the crystalline material confirmed spatial situation different from the NMR in solution. The signals that were shielded by ring current are shown in green. If the spatial situation in solution would be the same as in the crystal structures, only half of the signals would be shielded that does not correspond with the ^{1}H NMR spectra.

Study of J-dimer stability

Equilibrium constants covering monomerization of a sample and its association with pyridine (i.e., K_P constant, Chart S1) were determined from the titration of the samples (dissolved in toluene) with pyridine. Dye concentration of 1 µM (for **1**, **2**, **3**) or 10 µM (for **4**) was used. Eq. 1 was adopted from the literature based on the procedure described by Kobuke´s[4] and Torres´s[5] groups,:

$$A_M = \frac{2\varepsilon_M(A-A_M)}{2\varepsilon_M-\varepsilon_D} \qquad \text{(Eq. 1)}$$

, in which *A*, *ε, M, D* refer to absorbance, molar absorption coefficient, monomer of a compound and dimer of a compound, respectively. The value of ε_M was taken as the A at final titration point, value of ε_D as the A at initial point. A_M (calculated by Eq. 1 using A = 658, 659, 659 and 660 nm for **1**, **2**, **3** and **4**, respectively) was plotted as a function of concentration of pyridine (i.e., [P]) at all titration points. Obtained graphs were analyzed by GraphPad version 8.2 using non-linear regression, that provided appropriate K_P values. Fluorescence titration data were analyzed similarly using fluorescence emission maximum of dimer instead of A_M.

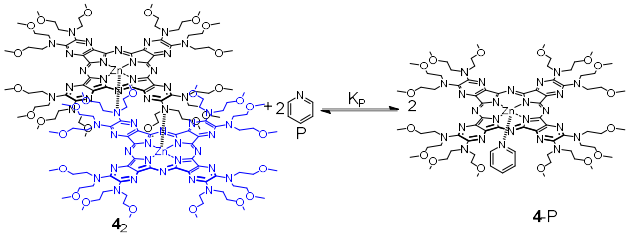

$$K_P = \frac{[\mathbf{4\text{-}P}]^2}{[(\mathbf{4})_2] \times [P]^2}$$

Chart S1: Scheme and equilibrium equation for reaction involving monomerization of the compound **4** and its association with pyridine.

Dimerization constant for **4** (K_D) was calculated after dilution of the sample in toluene from 100 µM to 0.1 µM (in some cases even to 0.01 µM) from a nonlinear regression of dependence of extinction coefficient at monomer maximum on the concentration of **4**.

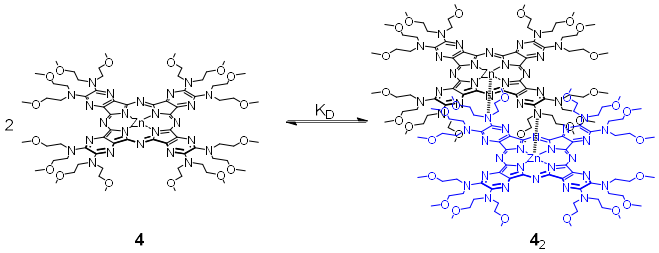

$$K_D = \frac{[(\mathbf{4})_2]}{[\mathbf{4}]^2}$$

Chart S2: Scheme and equilibrium equation of dimerization of compound **4**.

Association constant of compound **4** with pyridine (K_1) was calculated as follows: Eq. 2 below was derived based on the following equations of appropriate equilibrium constants of compound **4**:

$$K_P = \frac{[\mathbf{4}\text{-P}]^2}{[(\mathbf{4})_2] \times [P]^2} \qquad K_D = \frac{[(\mathbf{4})_2]}{[\mathbf{4}]^2} \qquad K_1 = \frac{[\mathbf{4}\text{-P}]}{[\mathbf{4}]\times[\text{P}]}$$

, where [4-P] states for concentration of complex of compound **4** with pyridine, [**4**] concertation of compound **4**, and [P] concentration of pyridine. By substitution in equation for K_D, we can get relation between K_1, K_D and K_P (Eq. 2):

$$K_D = \frac{[(\mathbf{4})_2]}{[\mathbf{4}]^2} = \frac{\frac{[\mathbf{4}\text{-P}]^2}{K_P[\text{P}]^2}}{\left(\frac{[\mathbf{4}\text{-P}]}{K_1\times[\text{P}]}\right)^2} = \frac{{K_1}^2}{K_P}$$

$$K_1 = \sqrt{K_D \times K_P} \qquad \text{(Eq. 2)}$$

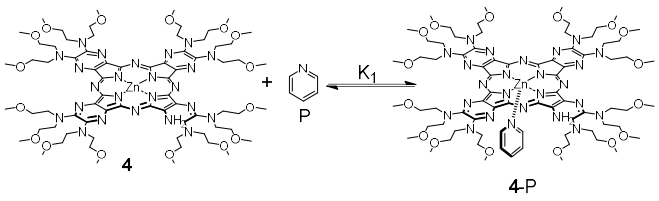

$$K_1 = \frac{[\mathbf{4}\text{-P}]}{[\mathbf{4}]\times[\text{P}]}$$

Chart S3: Scheme and definition of K_1 of compound **4**.

Study of J-dimer formation in ODN probes

Typical procedure was as follows: Appropriate amount of the stock solution of a probe was transferred into cuvette with hybridization buffer (600 µL) (*i.e.*, DNase I reaction buffer composed of 20 mm Tris-HCl (pH 8.4), 2 mm $MgCl_2$, 50 mm KCl) to get final concentration of 1 µM and fluorescence emission and absorption spectra were measured (excitation wavelength was 492 nm). Antisense strand **ODN-ant** (5 equivalents, *i.e.* its final concentration in cuvette was 5 µM) was added, the cuvette was heated at 75 °C for 10 min in water bath and then allowed to slowly (within 30 min) cool down to room temperature while protected from light. Fluorescence emission and absorption spectra of the hybridized duplex was then taken. After that, DNase I (1 U, Thermo Scientific) was added, and solution in the cuvette was left stirring for 20 minutes at room temperature protected from light. Fluorescence emission and absorption spectra of the mixture after cleavage were measured. This procedure was performed for each probe (**(ODN-1)$_2$**, **ODN-2**, (**F-ODN-1)$_2$** and **F-ODN-2**) and pyridine was added stepwise at different stages (always in a separate experiment) – with a probe before the addition of antisense **ODN-ant**, after hybridization step or after cleavage of the duplex (see schemes in Figs. 4, 5). Absorption and fluorescence emission spectra were taken after each addition of pyridine. Maximal concentration of pyridine was 2.5 M in all cases.

Quenching efficiency

Appropriate amount of the stock solution of a probe was transferred into cuvette with hybridization buffer (600 µL) to get final concentration of 50 nM and fluorescence emission spectrum was measured (excitation wavelength was 492 nm). Antisense strand **ODN-ant** (5 equivalents, *i.e.* its final concentration in cuvette was 250 nM) was added, the cuvette was heated at 75 °C for 10 min in water bath and then allowed to slowly (within 30 min) cool down to room temperature while protected from light. Fluorescence emission spectrum of the hybridized duplex was taken. After that, DNase I (1 U, Thermo Scientific) was added, and solution in the cuvette was left stirring for 20 minutes at room temperature protected from light. Fluorescence emission spectrum of the mixture after cleavage was measured. The quenching efficiency (QE) was calculated according to the following Eq. 3 using fluorescence intensity at emission maxima at 521 nm:

$$QE = \left(1 - \frac{F_x}{F_{max}}\right) \times 100 \qquad \text{Eq. 3}$$

in which F_{max} is the fluorescence intensity after full cleavage with DNase, and F_x is the fluorescence intensity in a random coil (for static quenching) or fluorescence intensity of the hybridized duplex (for FRET). All measurements were performed in triplicate and the presented values represent the mean value.

Real time PCR

Real time PCR was performed using a Real-Time PCR Detection System CFX96T (Bio-Rad) with a gb Ideal master mix (Generi Biotech), and the temperature profile of the reaction was as follows: initial denaturation at 95°C for 3 min and 50 cycles of denaturation at 95°C for 15 s, followed by annealing and elongation at 60°C for 30 s. A plasmid standard was prepared using molecular cloning described previously.[6] The calibration curves for each probe were obtained by measuring a series of decimally diluted plasmid standards (the numbers of copies in the reaction were in the 10^7-10^2 range). The probes and primers were based on a quantification assay for the SLCO2B1 transporter gene. The primers for real-time PCR were synthesized by Generi Biotech with the following sequences: forward primer: GTCTCACCCACACACCCTC, reverse primer: ATGCCCACAGCCAAAGTCT. The concentration of the **F-ODN-2** probe was 150 nM. All calibration measurements were performed in triplicate for each concentration of the standard and the probes.

Determination of melting temperature

The determination of melting temperature (T_m) was performed on Real-Time PCR Detection System CFX96T (Bio-Rad). The antisense ODN modified at 5'-end by HEX (0.3 µM, sequence: HEX-

TCACTCCTCTTAGGATGAGCATGA) was mixed with the studied **ODN-1**, **ODN-2, F-ODN-1** or **F-ODN-2** (0.4 μM), heated to 95°C and cooled down to 40°C. The formed duplex was subsequently heated (40-80°C, 0.2 °C / 5s) and fluorescence of HEX was measured (λ_{exc} = 515-535 nm, λ_{em} = 560-580 nm). The derivative of the dependence of fluorescence intensity on time was used to determine the T_m of each duplex. The experiment was performed in triplicate and the data in the manuscript are expressed as mean ± standard deviation.

Characterization of J-dimers in organic solvents

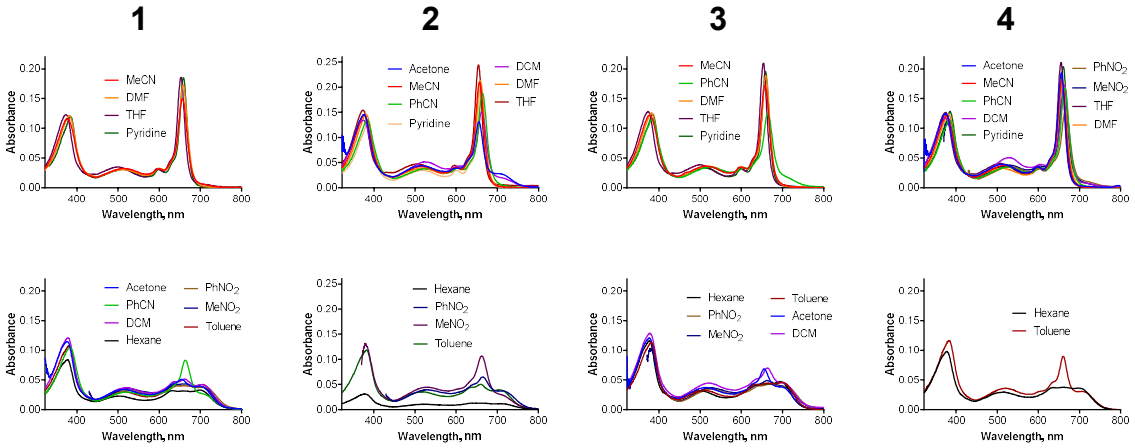

Fig. S7. Absorption spectra of compounds **1**-**4** (1 μM) in different solvents. Upper row shows the spectra where the compounds are predominantly monomeric, lower row where they form J-dimers.

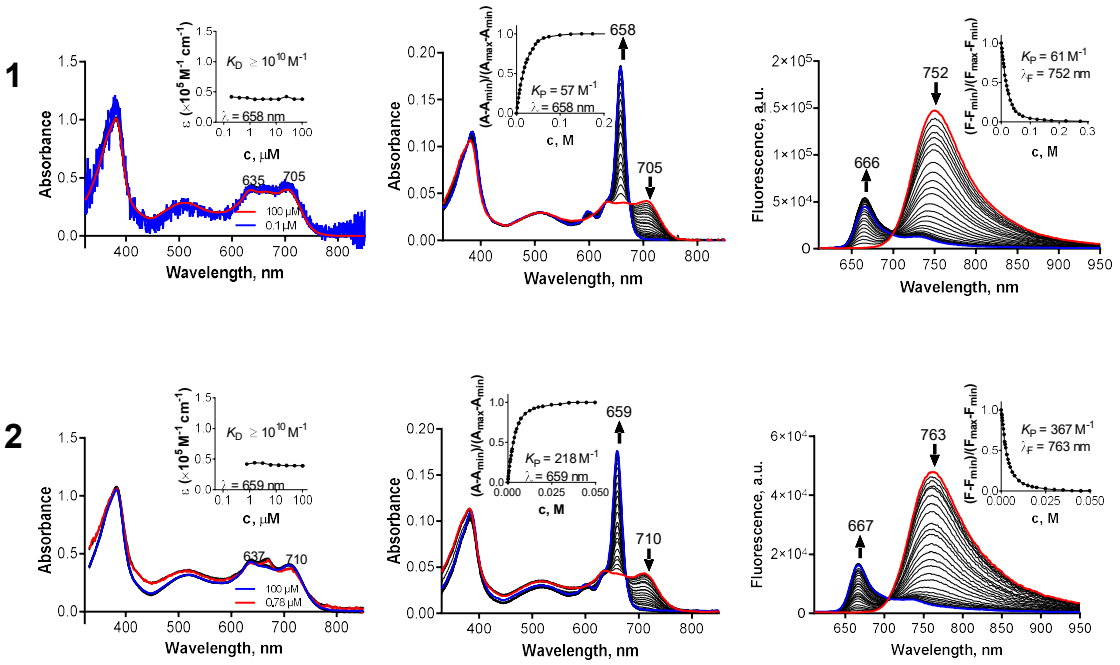

Fig. S8 Determination of K_D and K_P values for compounds **1** and **2**.

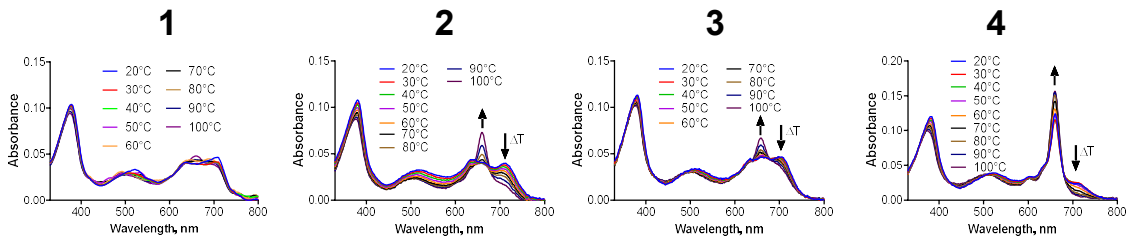

Fig. S9. Spectral changes of toluene solutions of **1**-**4** (1 μM) with increasing temperature.

Photophysics

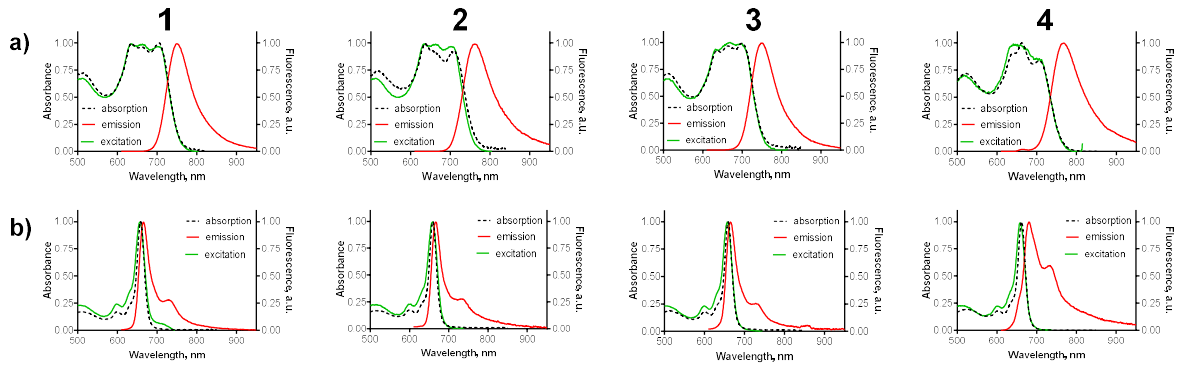

Fig. S10 Normalized absorption (black, dashed), emission (red) and excitation (green) spectra of compounds **1** – **4** in toluene (a) and toluene with 250 mM pyridine (b).

Characterization of J-dimers in ODN probes

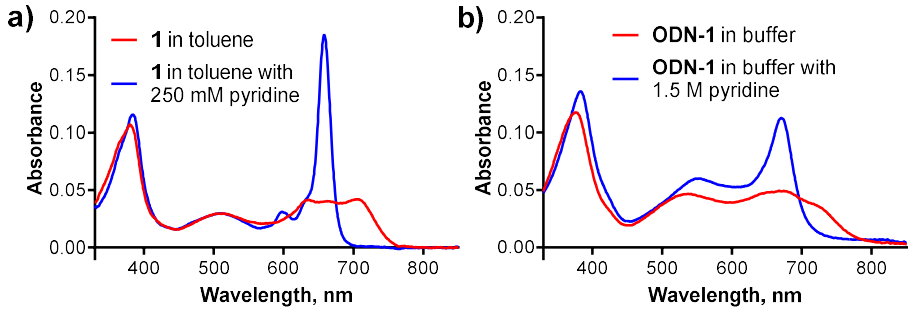

Fig. S11. Absorption spectra (1 µM) of **1** (a) in toluene (red, J-dimer) and in toluene with 250 mM pyridine (blue, monomer) and **ODN-1** (b) in hybridization buffer (red, J-dimer) and in hybridization buffer with 1.5 M pyridine (blue, monomer).

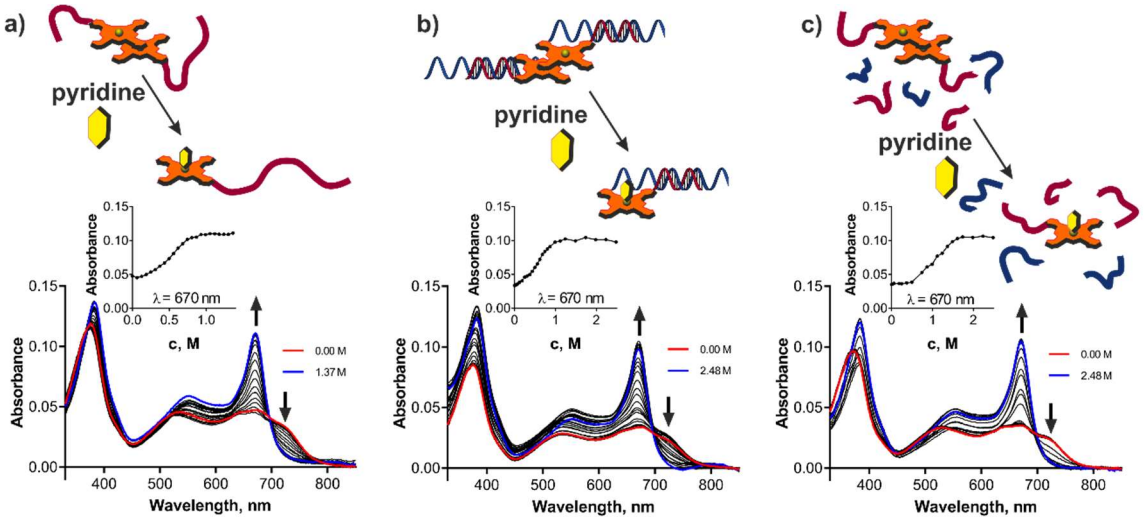

Fig. S12. Changes in absorption spectra during addition of pyridine into 1 μM solution of the **(ODN-1)$_2$** probe in hybridization buffer. a) Addition to probe alone in solution. b) Addition to duplex **(ODN-1)**$_2$-**ODN-ant.** c) Addition to the fragments that arose after cleavage of the duplex by DNase.

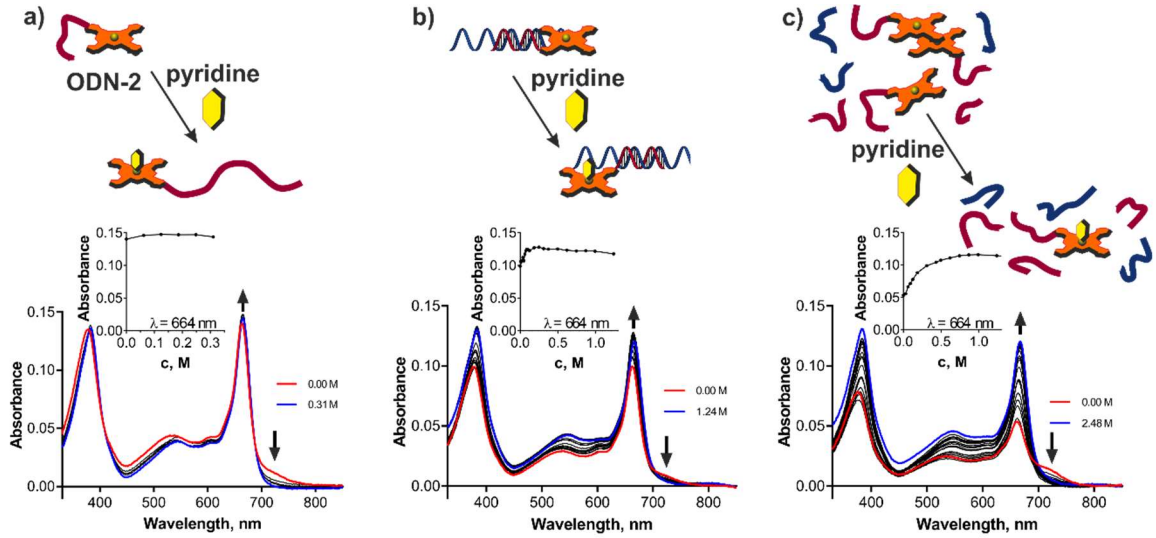

Fig. S13. Changes in absorption spectra during addition of pyridine into 1 μM solution of the **ODN-2** probe in hybridization buffer. a) Addition to probe alone in solution. b) Addition to duplex **ODN-2-ODN-ant.** c) Addition to the fragments that arose after cleavage of the duplex by DNase.

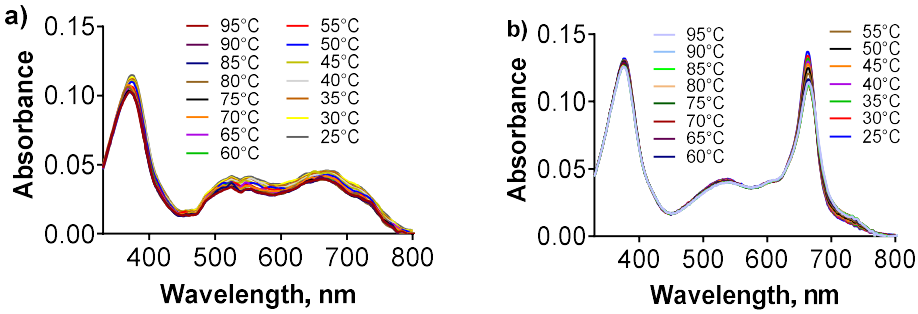

Fig. S14. Spectral changes of **(ODN-1)$_2$** (a) and **ODN-2** (b) in hybridization buffer with increasing temperature.

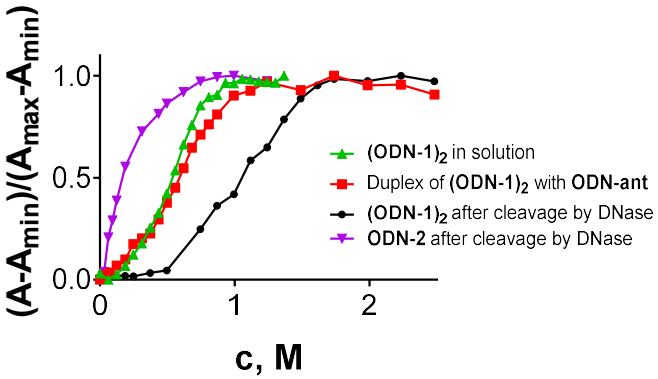

Fig. S15. Dependence of absorbance at 673 nm (for **ODN-1**)or 667 nm (for **ODN-2**) on the amount of added pyridine.

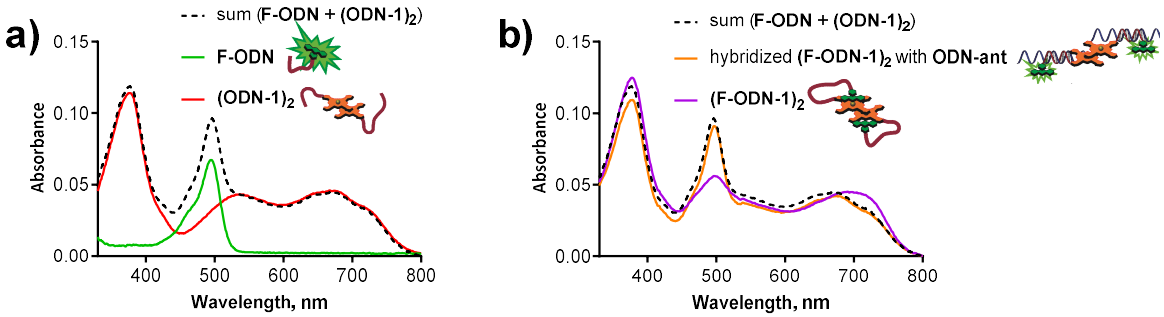

Fig. S16. a) Absorption spectra of 1 µM solutions of **(ODN-1)$_2$** (red), **F-ODN** (green) in hybridization buffer and a mathematical sum of these spectra (black, dashed). b) Absorption spectra of 1 µM solutions of heterotetramer **(F-ODN-1)$_2$** (magenta), dsDNA of hybridized **(F-ODN-1)$_2$** with **ODN-ant** (orange) in hybridization buffer and the mathematical sum of spectra from figure a) (black, dashed).

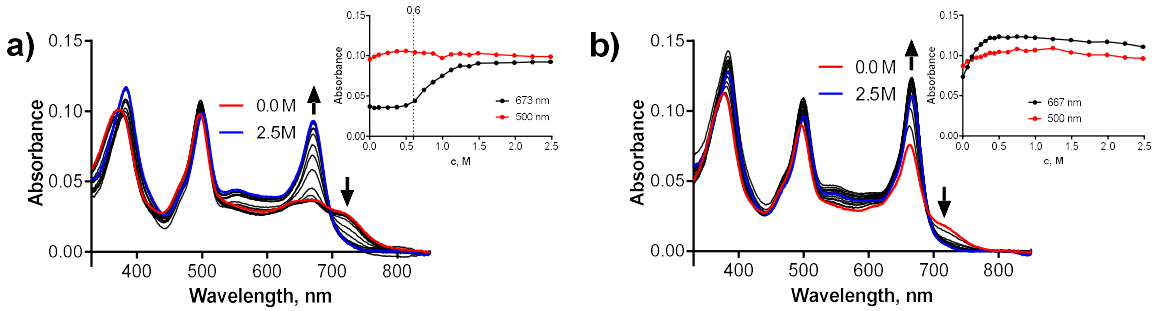

Fig. S17. Absorption changes of (**F-ODN-1**)$_2$ (a) and **F-ODN-2** (b) at concentration of 1 µM in hybridization buffer after addition of pyridine to the fragments that arose after cleavage of the duplex by DNase. Insets: Dependence of absorbance at 500 nm (red, corresponds to fluorescein) and 673 nm or 667 nm (black, corresponds to monomeric species of AzaPcs) on the added pyridine.

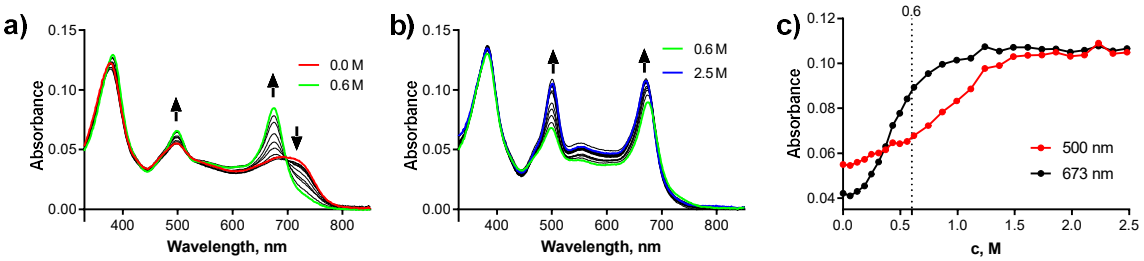

Fig. S18. a) Absorption changes in (**F-ODN-1**)$_2$ at concentration of 1 µM in hybridization buffer during addition of pyridine (up to 0.6 M). b) Absorption changes in (**F-ODN-1**)$_2$ at concentration of 1 µM in hybridization buffer during addition of pyridine (from 0.6 M to 2.5 M). c) Dependence of absorbance at 500 nm (red, corresponds to fluorescein) and 673 nm (black, corresponds to monomeric species of AzaPc).

NMR spectra

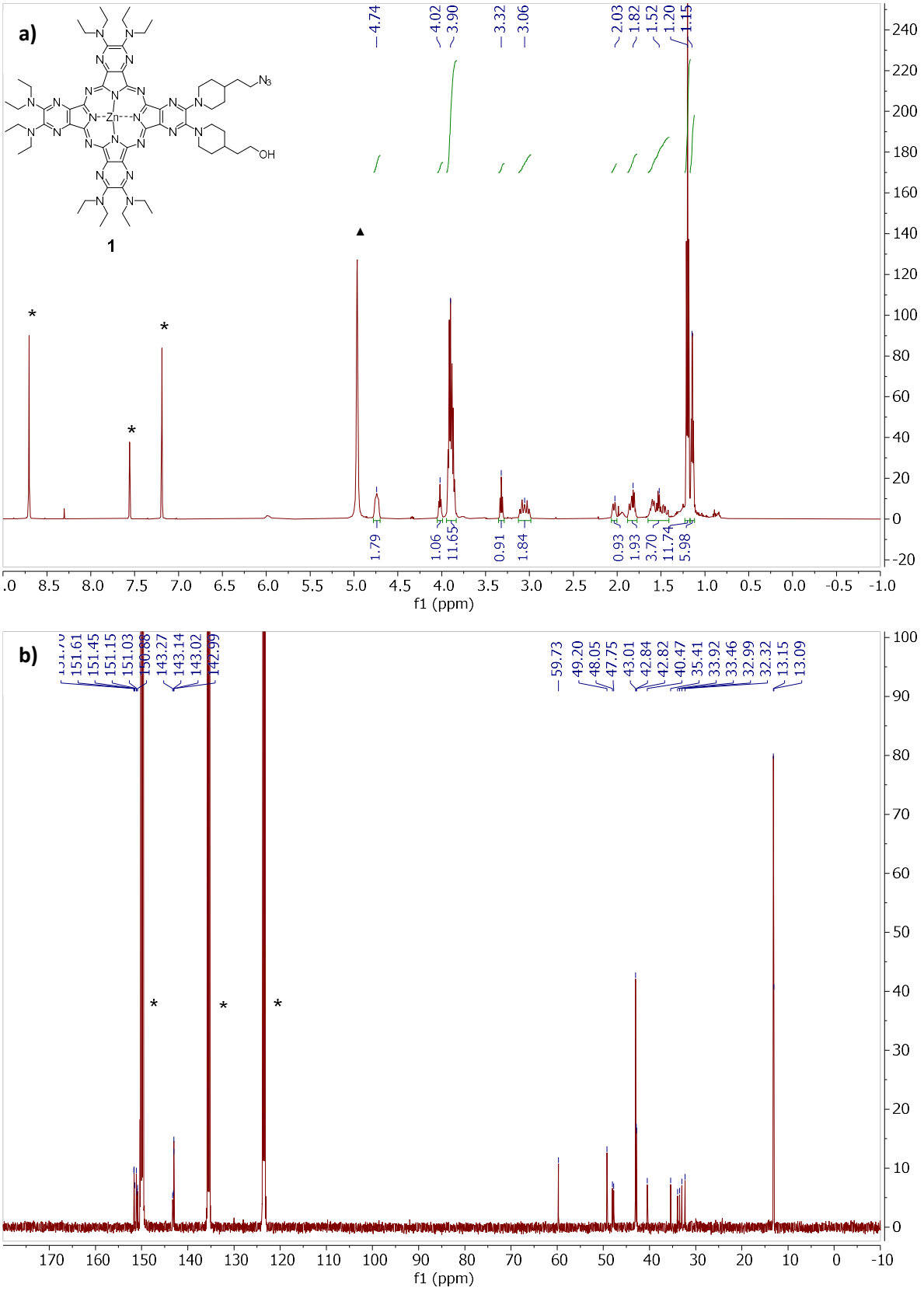

Fig. S19: ^{1}H NMR (500 MHz) (a) and ^{13}C NMR (126 MHz) (b) spectra of compound **1** in pyridine-d_5. Asterisk (*) and triangle (▲) indicate residuals of non-deuterated solvent and water, respectively.

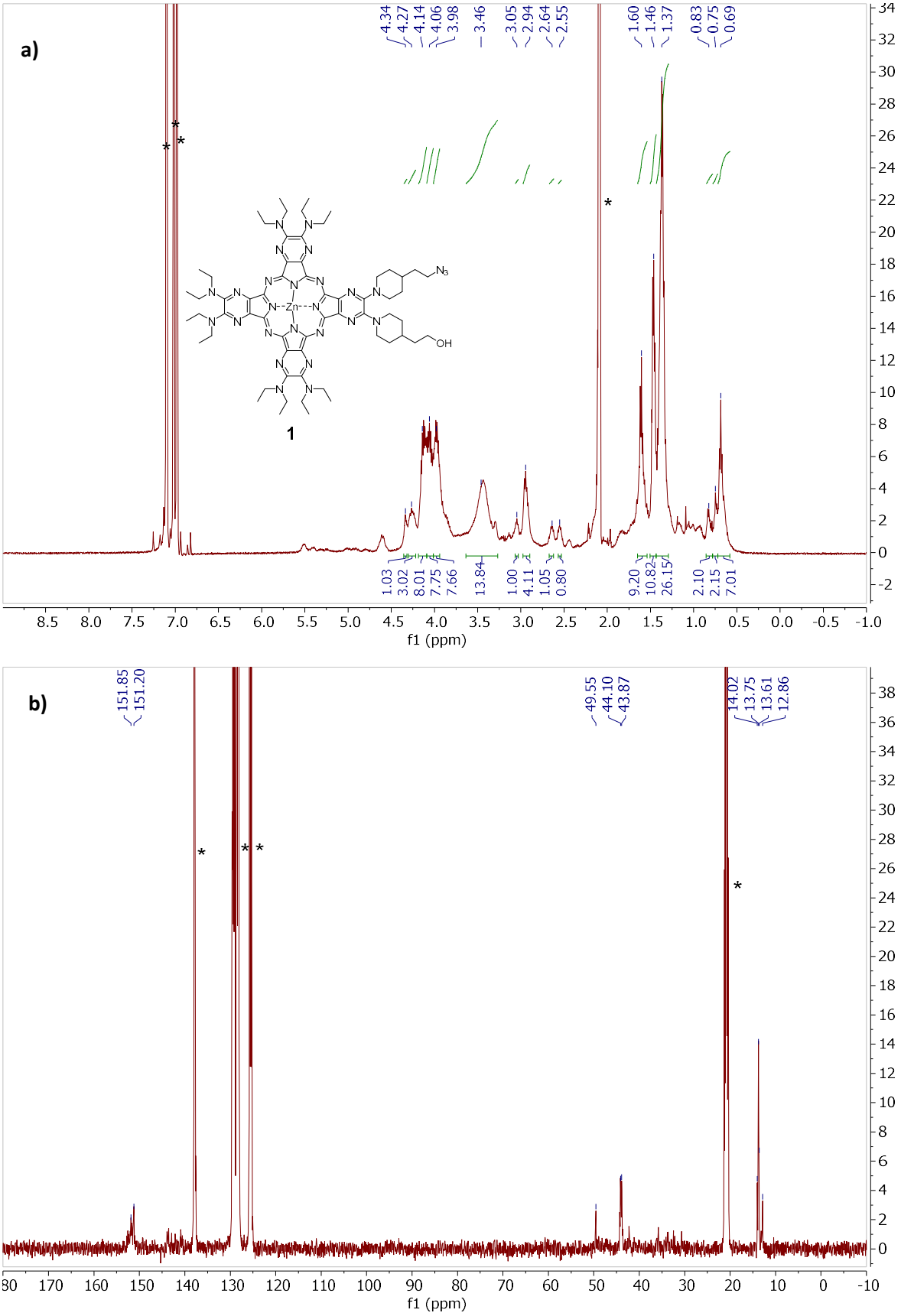

Fig. S20: ^{1}H NMR (500 MHz) (a) and ^{13}C NMR (126 MHz) (b) spectra of compound **1** in toluene-d_8. Asterisk (*) indicates residuals of non-deuterated solvent.

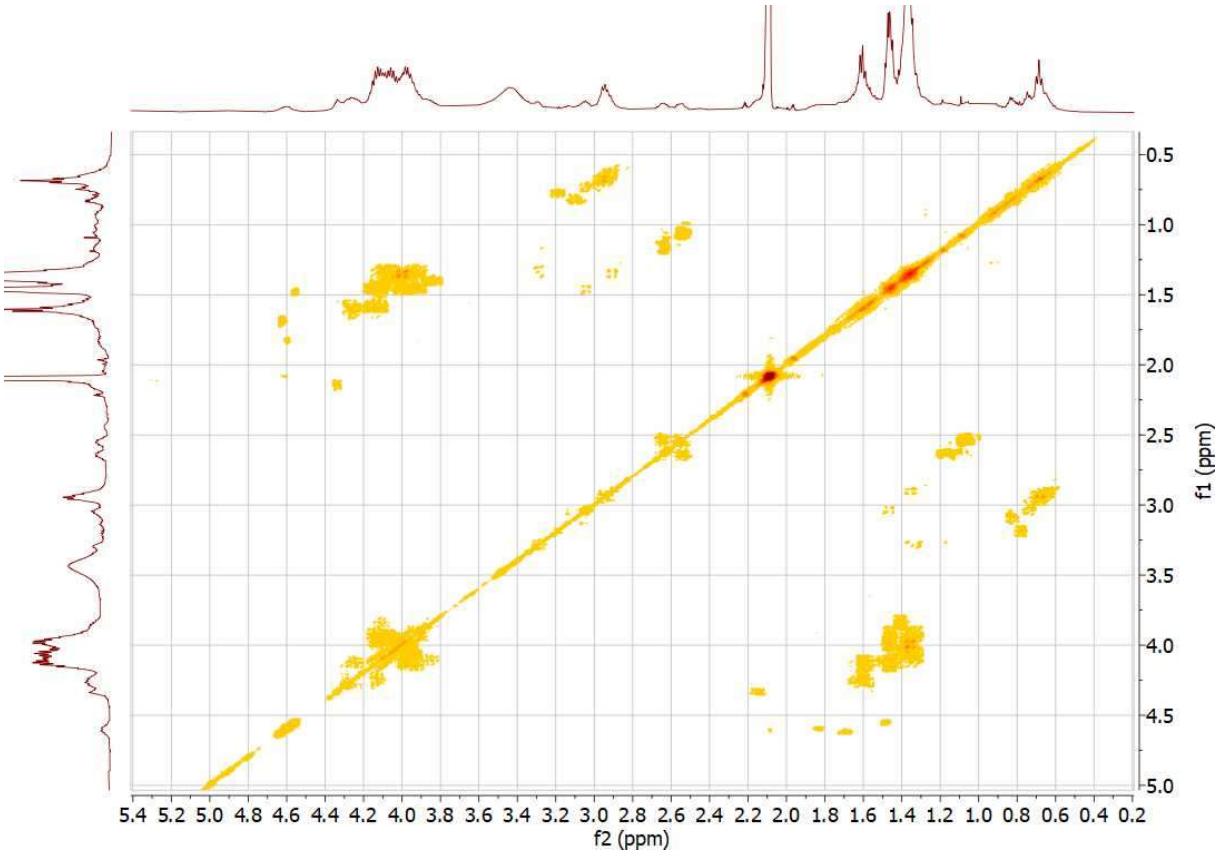

Fig. S21: ^{1}H-^{1}H NMR COSY spectrum of compound **1** in toluene-d_8.

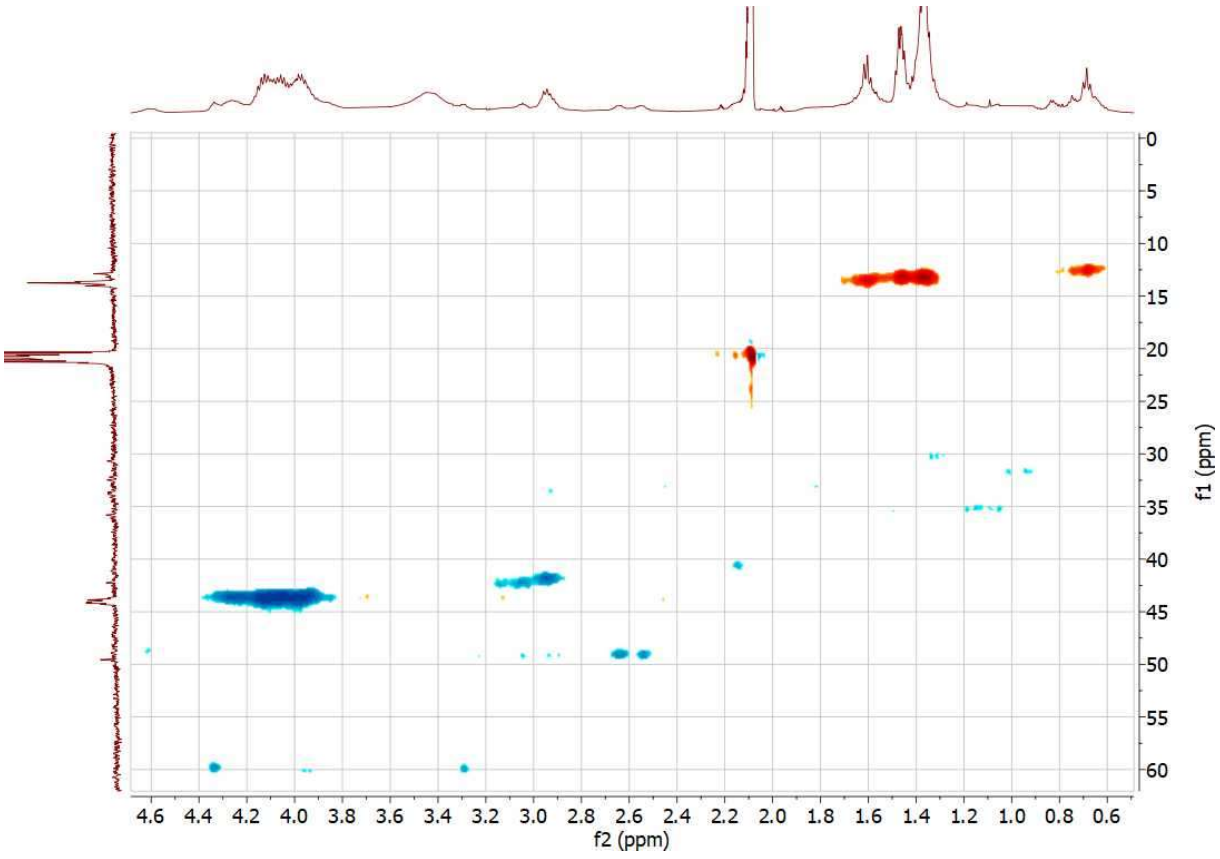

Fig. S21: ^{1}H-^{13}C NMR HSQC spectrum of compound **1** in toluene-d_8.

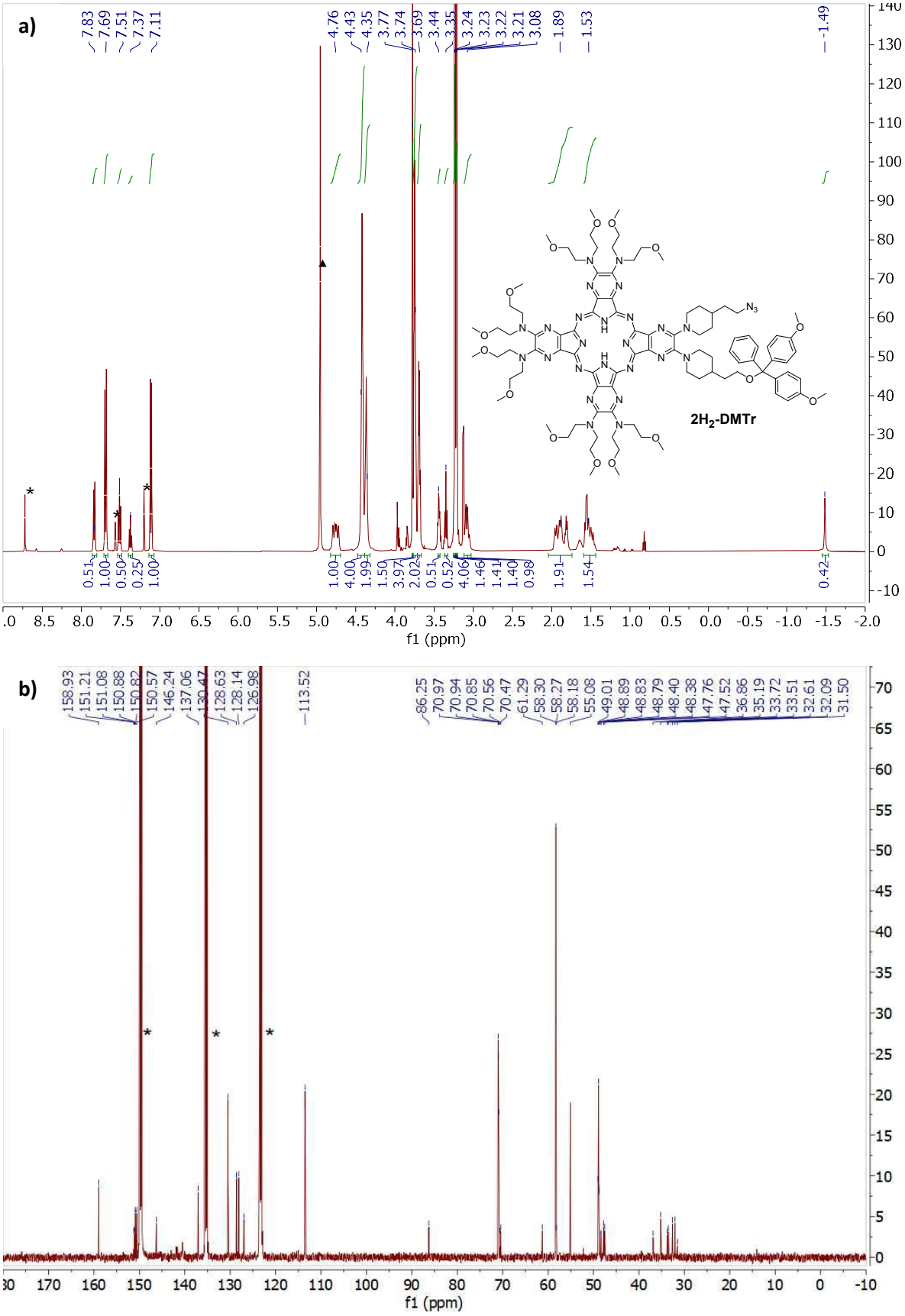

Fig. S22: ^{1}H NMR (500 MHz) (a) and ^{13}C NMR (126 MHz) (b) spectra of compound **2H$_2$-DMTr** in pyridine-*d*$_5$. Asterisk (*) and triangle (▲) indicate residuals of non-deuterated solvent and water, respectively.

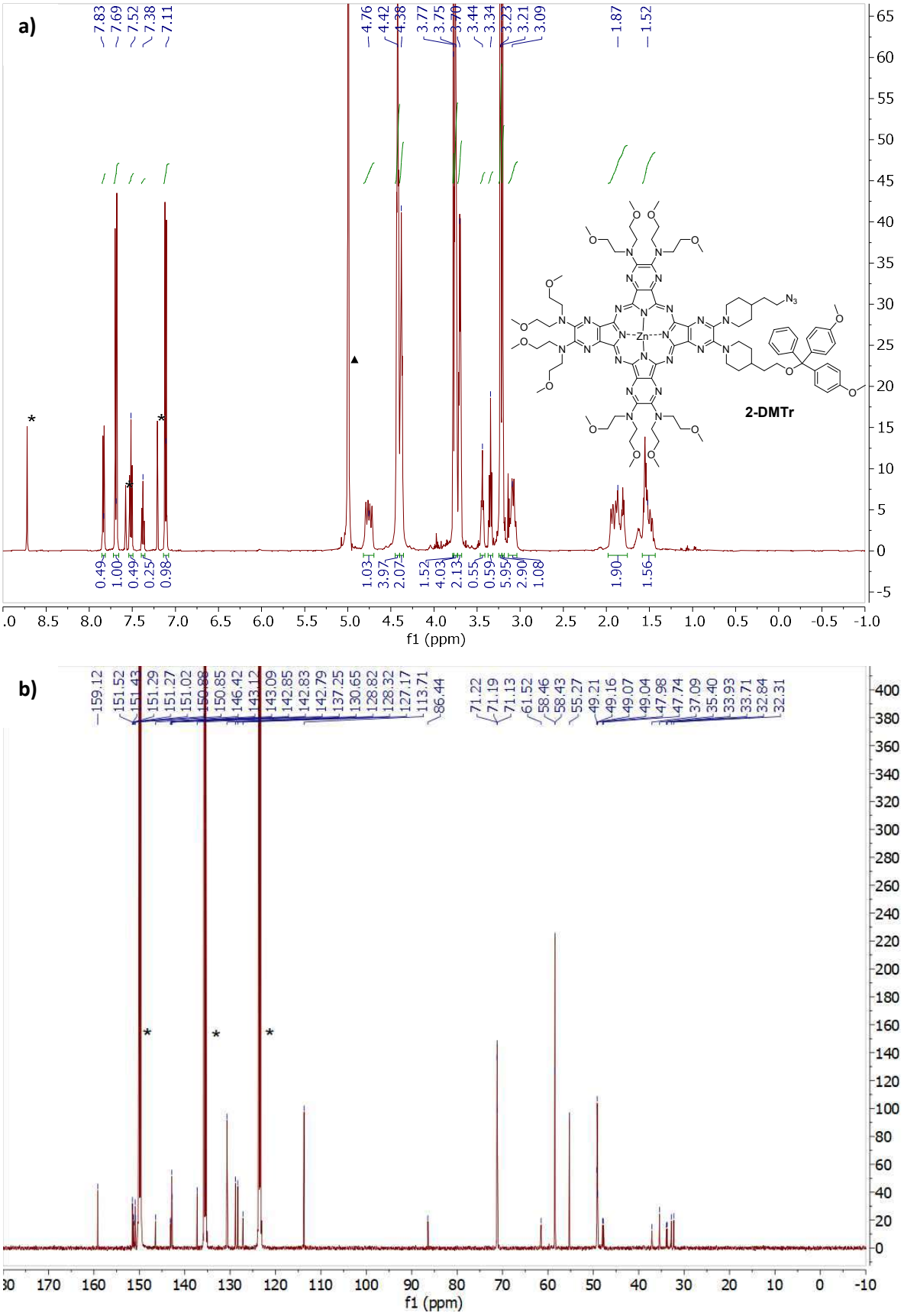

Fig. S23: ^{1}H NMR (500 MHz) (a) and ^{13}C NMR (126 MHz) (b) spectra of compound **2-DMTr** in pyridine-d_5. Asterisk (*) and triangle (▲) indicate residuals of non-deuterated solvent and water, respectively.

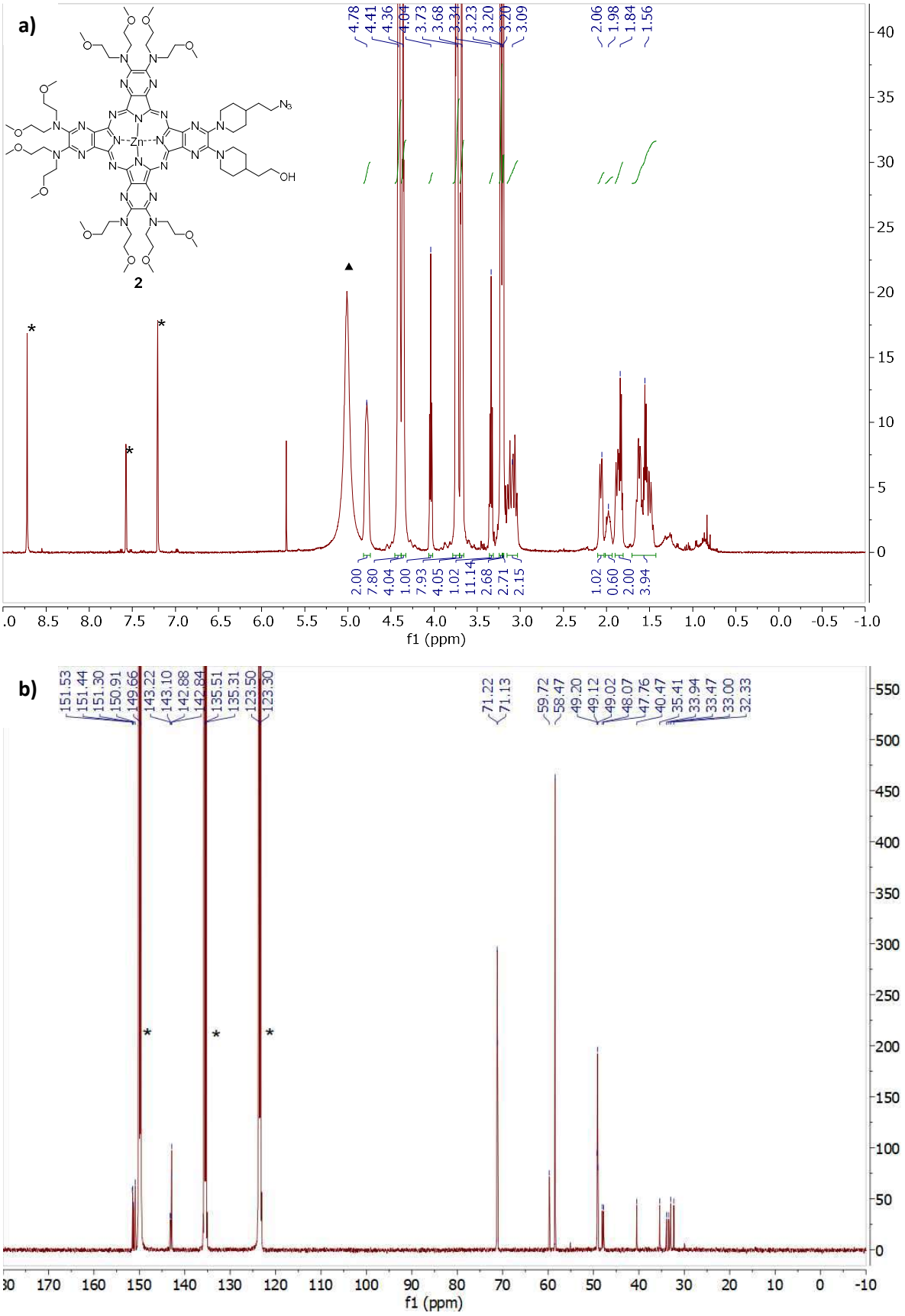

Fig. S24: ^{1}H NMR (500 MHz) (a) and ^{13}C NMR (126 MHz) (b) spectra of compound **2** in pyridine-d_5. Asterisk (*) and triangle (▲) indicate residuals of non-deuterated solvent and water, respectively.

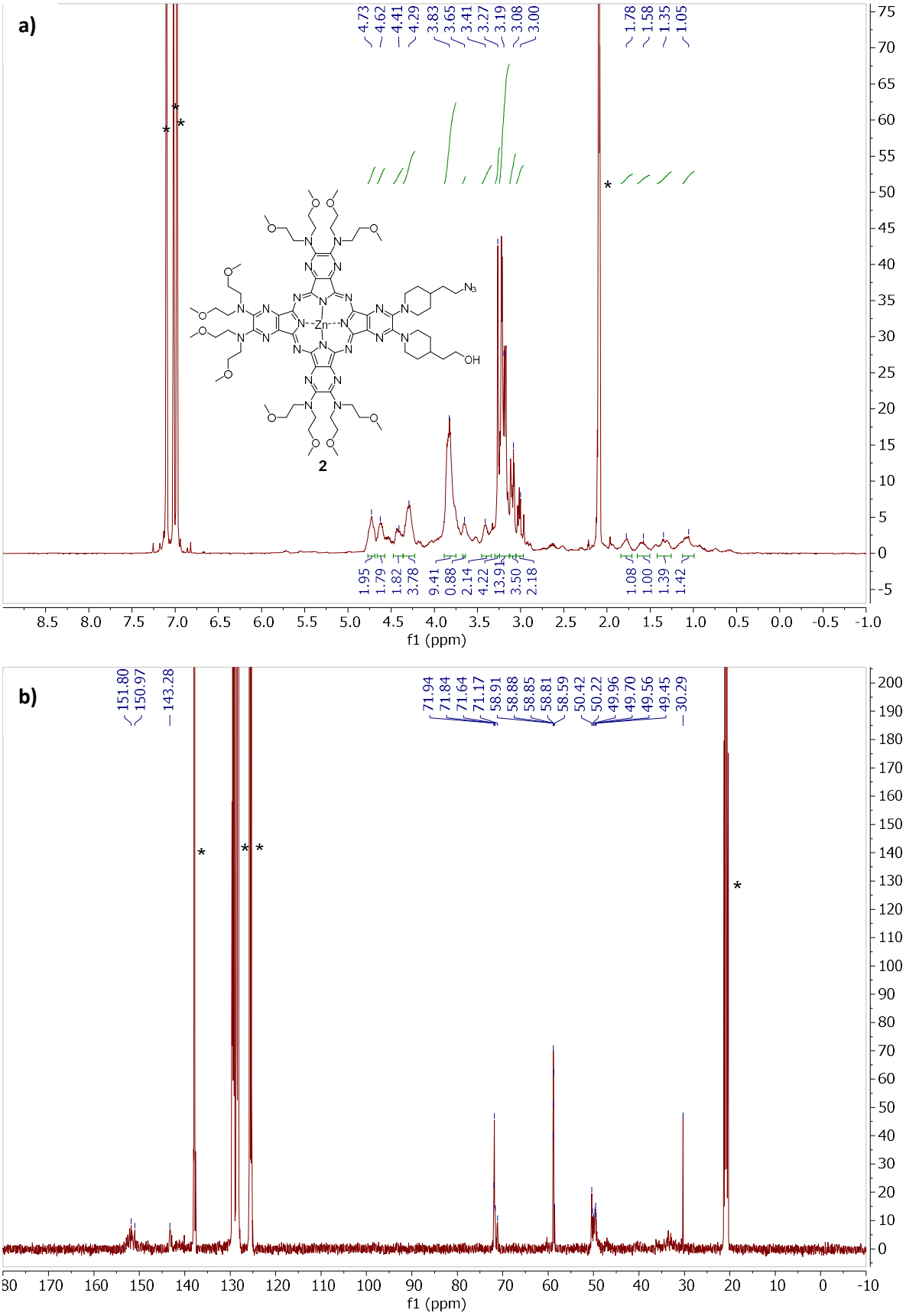

Fig. S25: ^{1}H NMR (500 MHz) (a) and ^{13}C NMR (126 MHz) (b) spectra of compound **2** in toluene-d_8. Asterisk (*) indicates residuals of non-deuterated solvent.

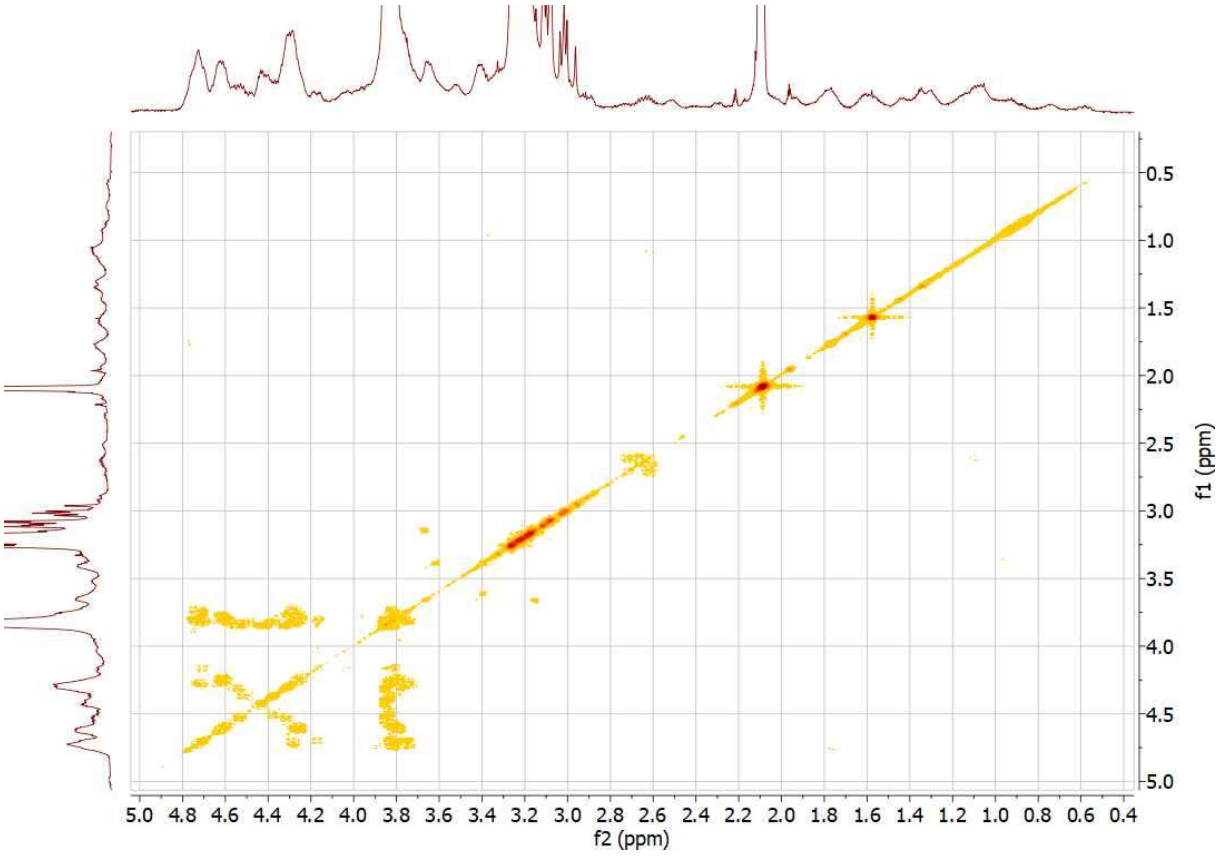

Fig. S26: ^{1}H-^{1}H NMR COSY spectrum of compound **2** in toluene-d_8.

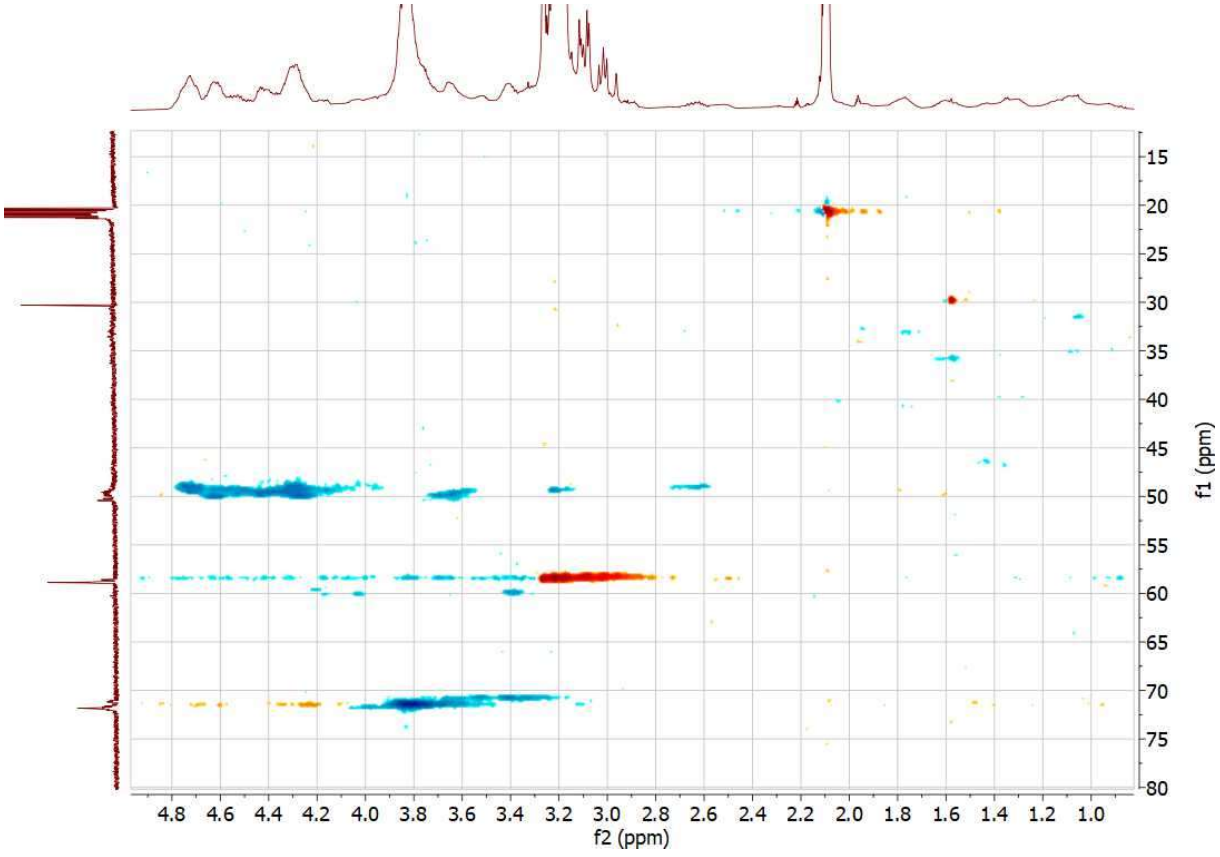

Fig. S27: ^{1}H-^{13}C NMR HSQC spectrum of compound **2** in toluene-d_8.

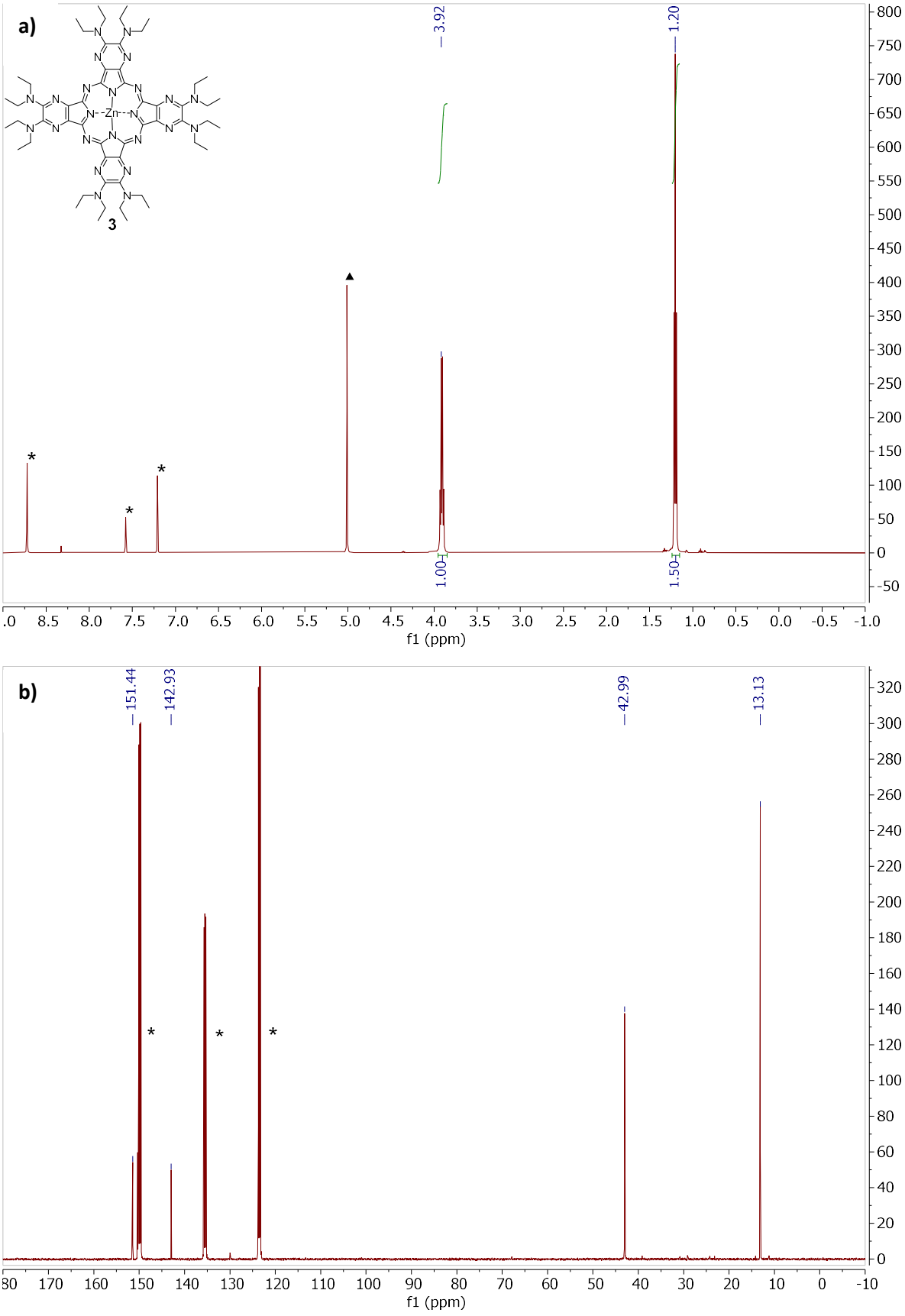

Fig. S28: ^{1}H NMR (500 MHz) (a) and ^{13}C NMR (126 MHz) (b) spectra of compound **3** in pyridine-d_5. Asterisk (*) and triangle (▲) indicate residuals of non-deuterated solvent and water, respectively.

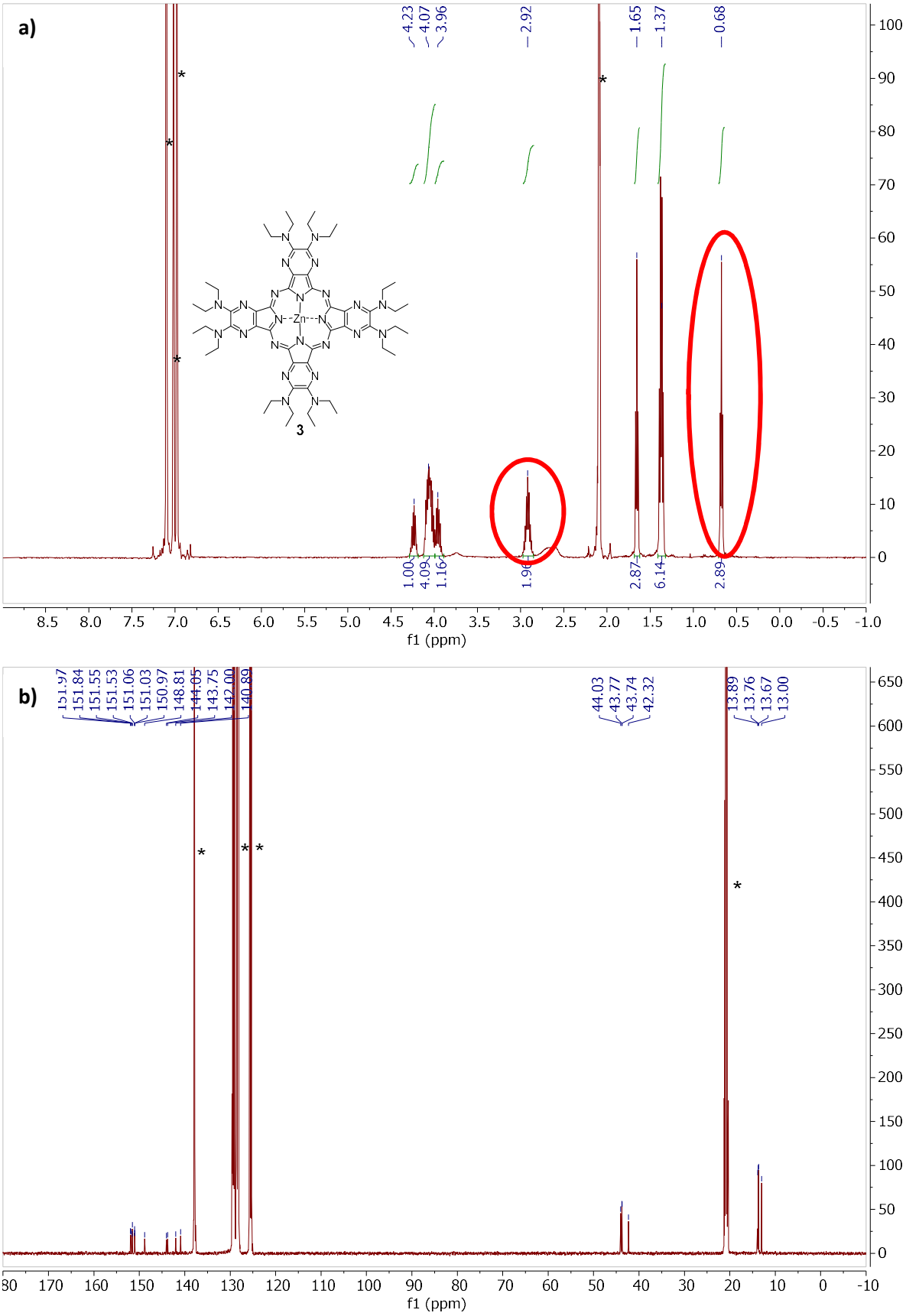

Fig. S29: ^{1}H NMR (500 MHz) (a) and ^{13}C NMR (126 MHz) (b) spectra of compound **3** in toluene-d_8. Asterisk (*) indicates residuals of non-deuterated solvent. Red circles indicate signals shielded by the ring-current effect.

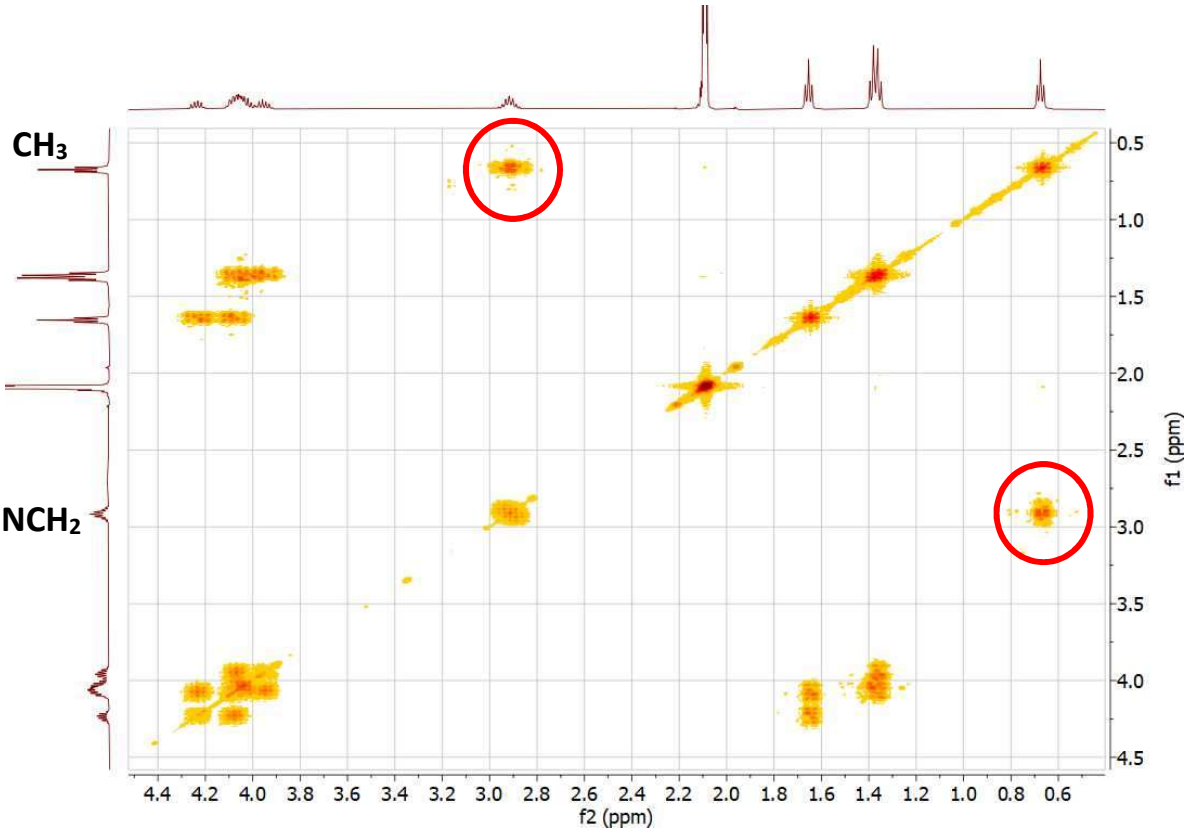

Fig. S30: ^{1}H-^{1}H NMR COSY spectrum of compound **3** in toluene-d_8. Red circles indicate signals shielded by the ring-current effect.

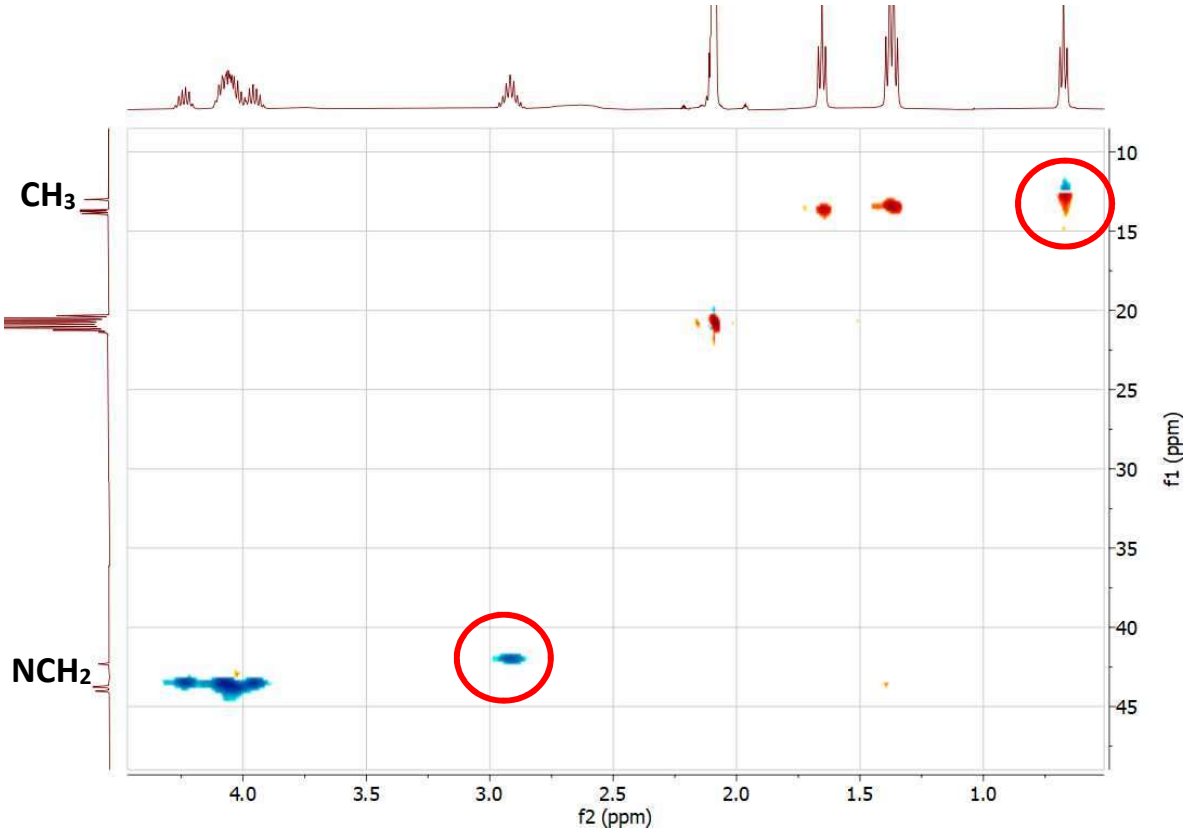

Fig. S31: ^{1}H-^{13}C NMR HSQC spectrum of compound **3** in toluene-d_8. Red circles indicate signals shielded by the ring-current effect.

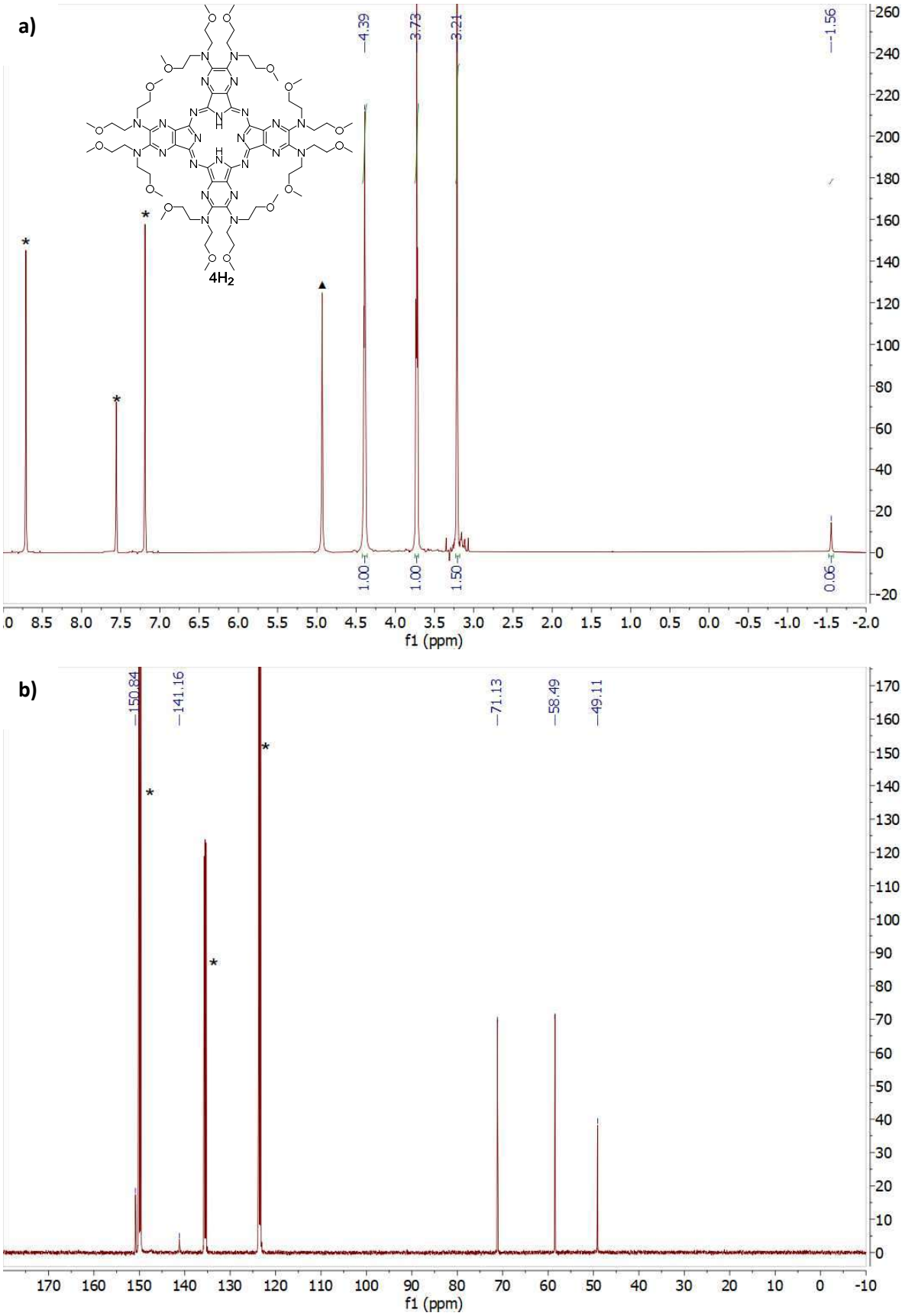

Fig. S32: ^{1}H NMR (500 MHz) (a) and ^{13}C NMR (126 MHz) (b) spectra of compound **4H₂** in pyridine-d_5. Asterisk (*) and triangle (▲) indicate residuals of non-deuterated solvent and water, respectively.

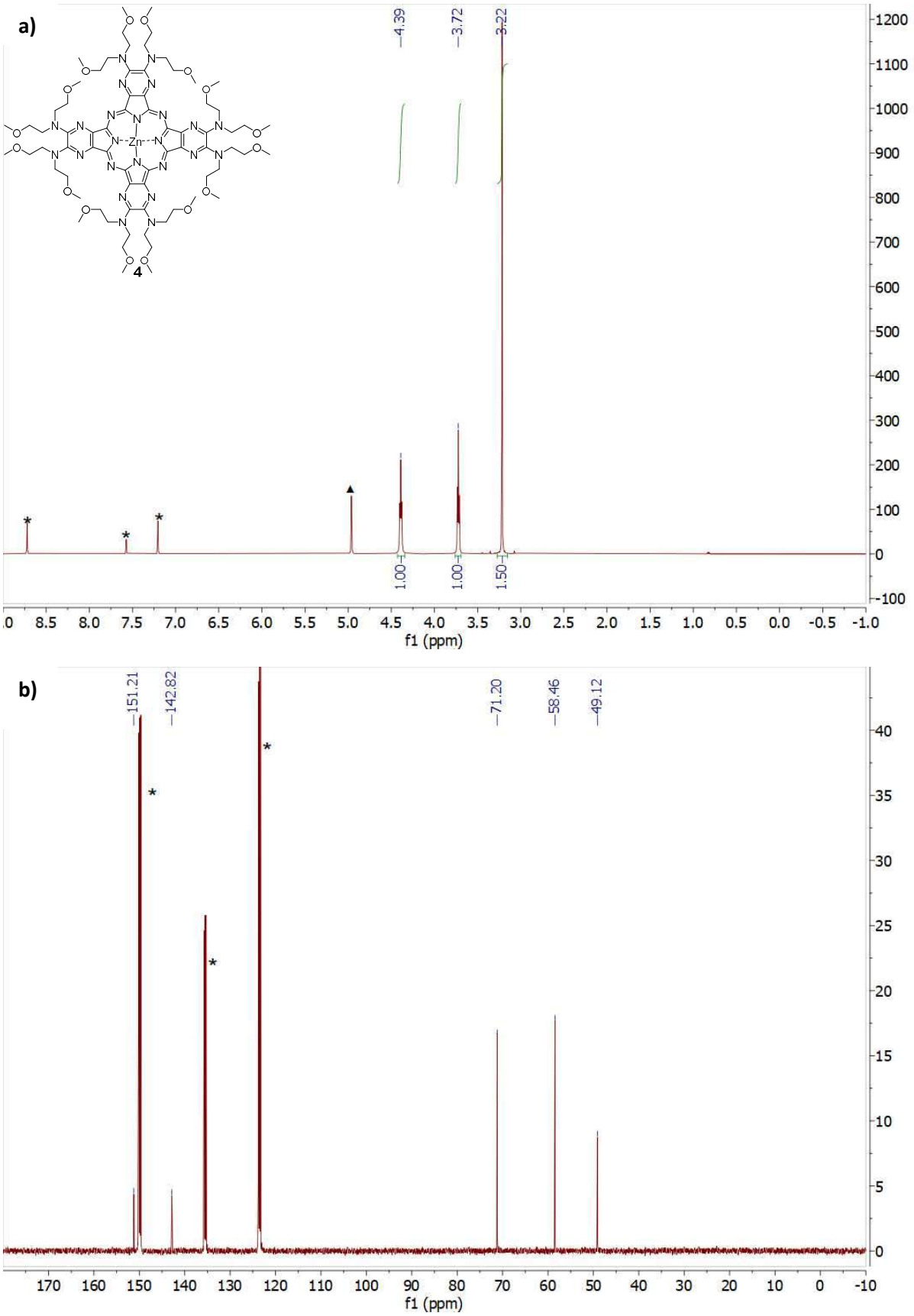

Fig. S33: ^{1}H NMR (500 MHz) (a) and ^{13}C NMR (126 MHz) (b) spectra of compound **4** in pyridine-d_5. Asterisk (*) and triangle (▲) indicate residuals of non-deuterated solvent and water, respectively

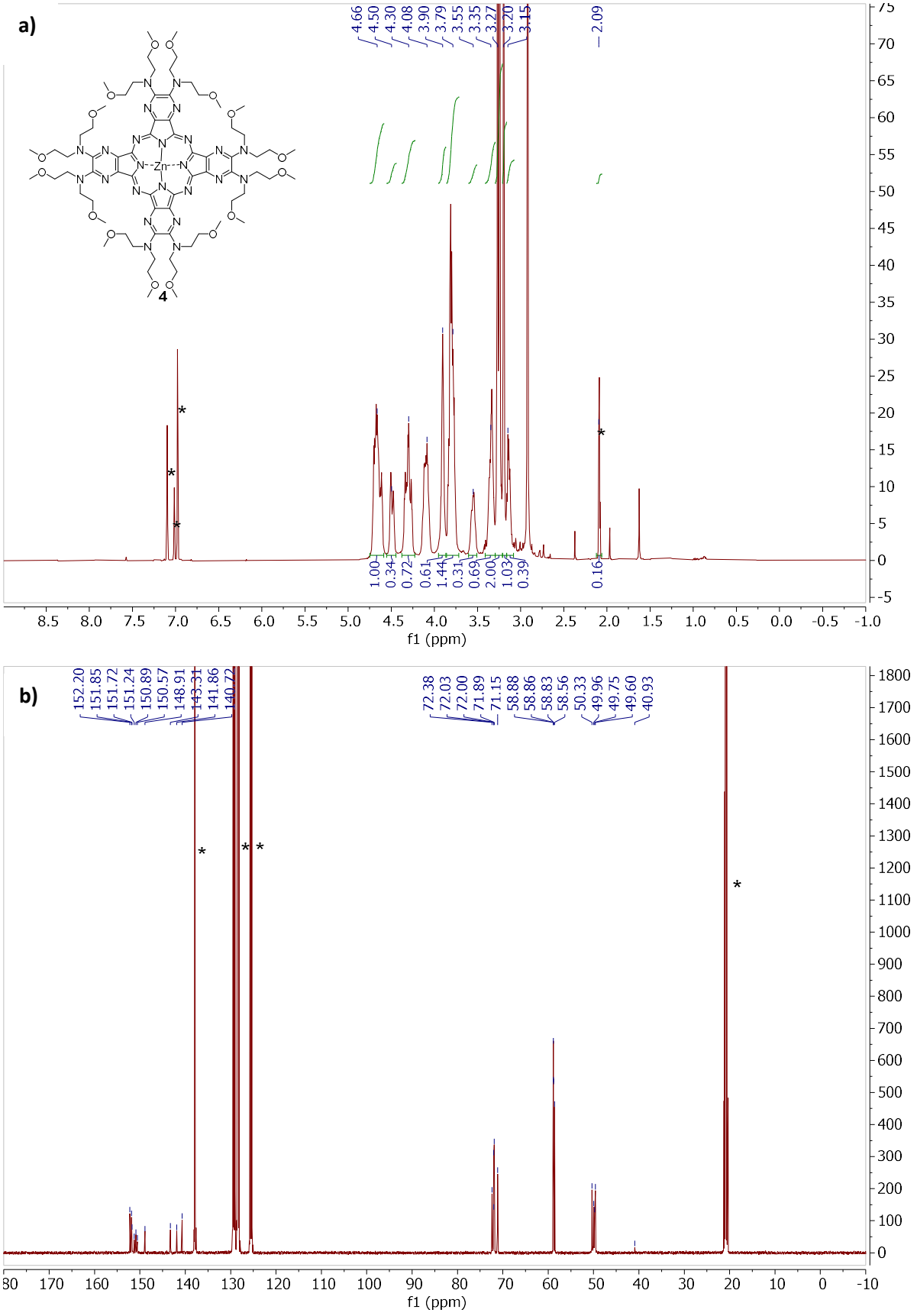

Fig. S34: ^{1}H NMR (500 MHz) (a) and ^{13}C NMR (126 MHz) (b) spectra of compound **4** in toluene-d_8. Asterisk (*) indicates residuals of non-deuterated solvent.

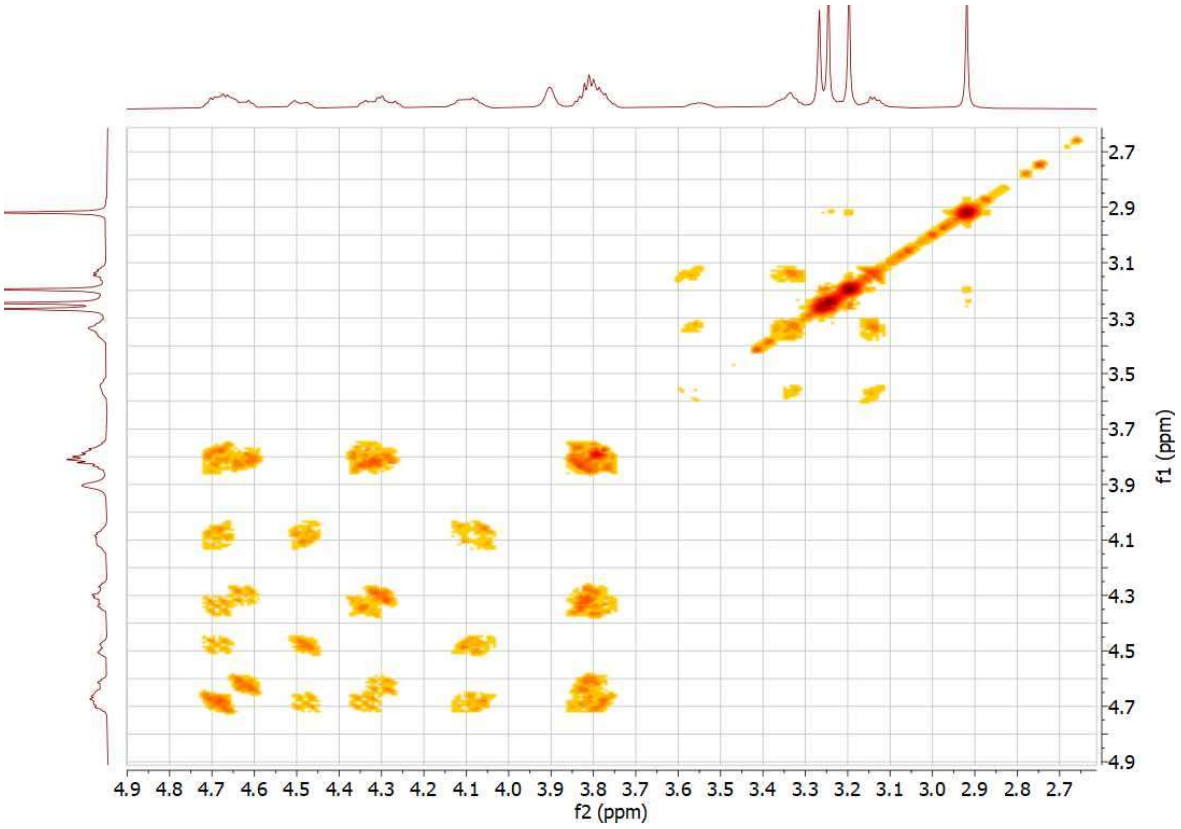

Fig. S35: ^{1}H-^{1}H NMR COSY spectrum of compound **4** in toluene-d_8.

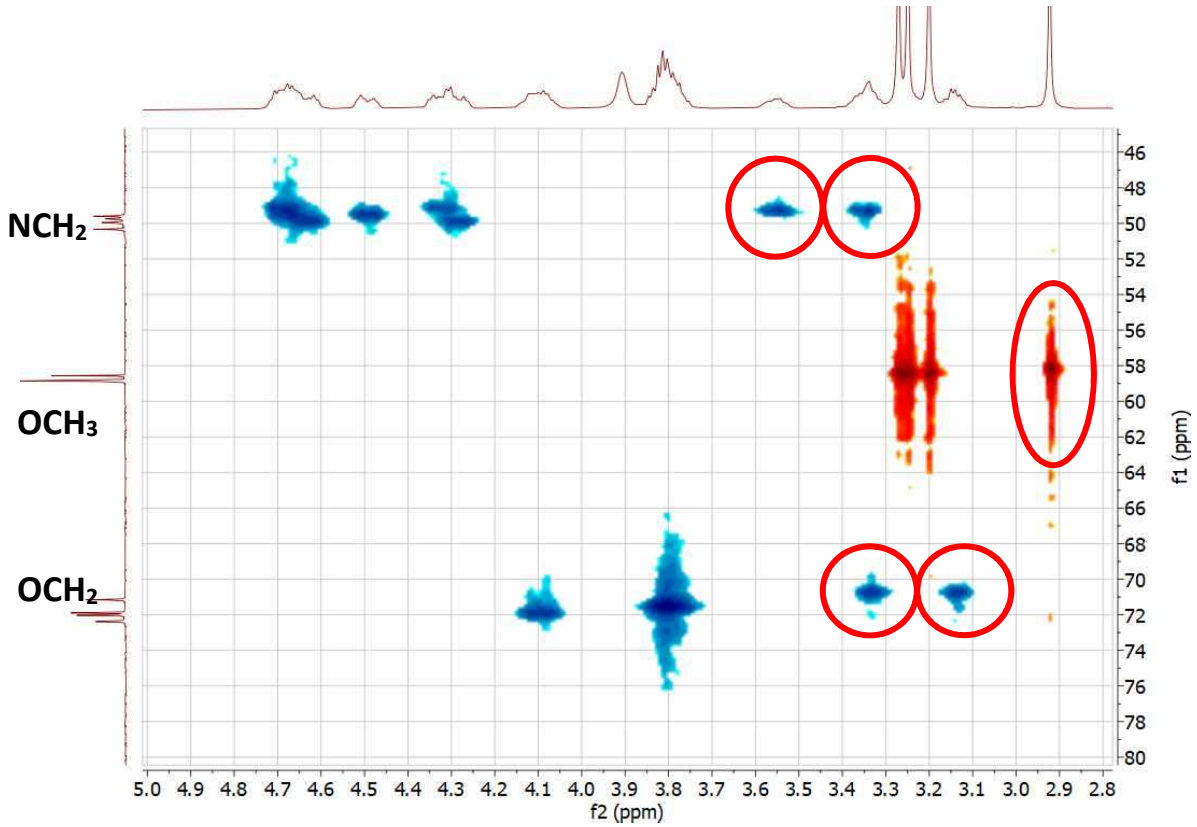

Fig. S36: ^{1}H-^{13}C NMR HSQC spectrum of compound **4** in toluene-d_8. Red circles indicate signals shielded by the ring-current effect.

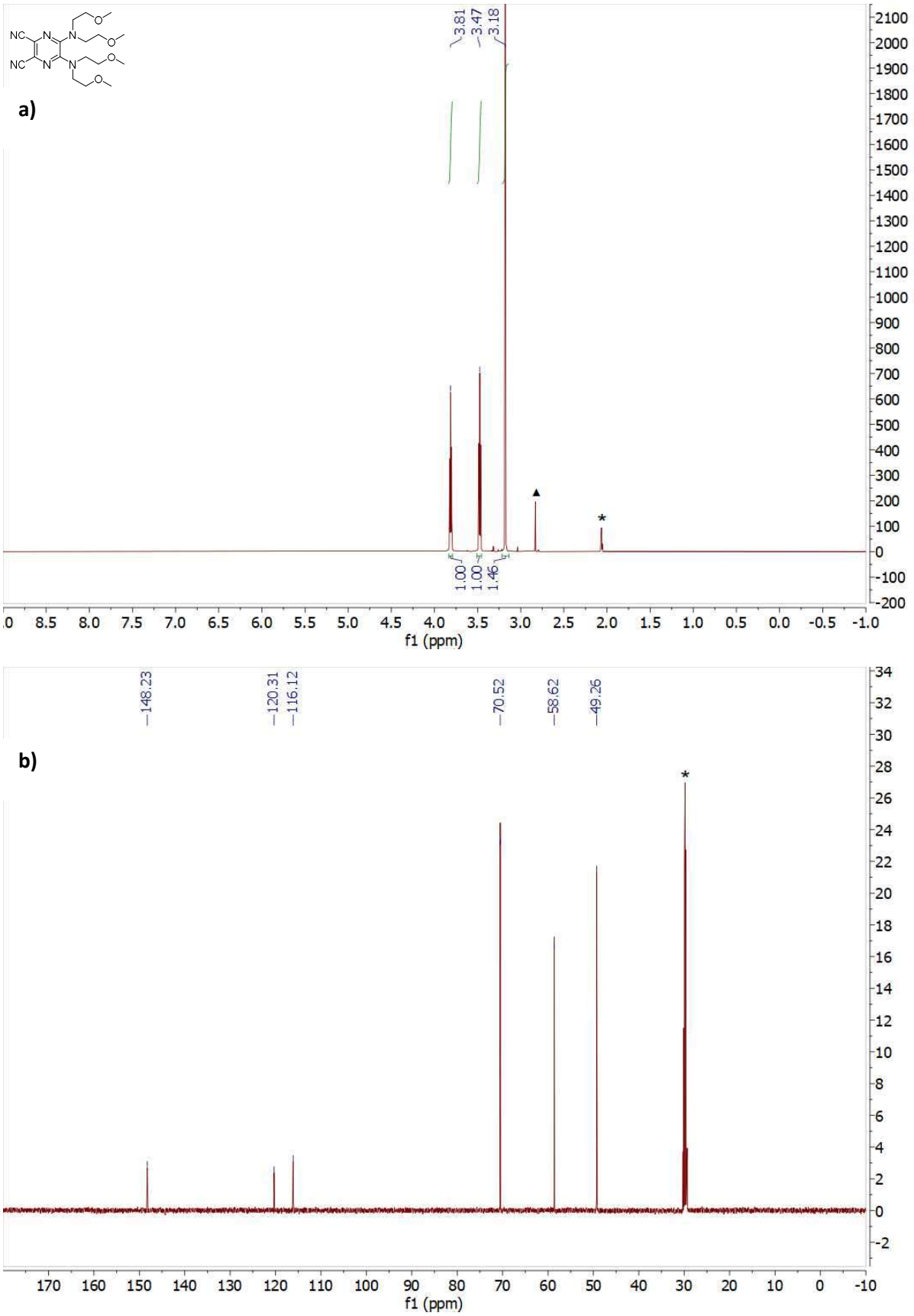

Fig. S37: ^{1}H NMR (500 MHz) (a) and ^{13}C NMR (126 MHz) (b) spectra of compound **5** in aceton-d_6. Asterisk (*) and triangle (▲) indicate residuals of non-deuterated solvent and water, respectively.

Crystallography - Experimental

Full-sets of diffraction data for **3** and **4** were collected at 150(2)K with a Bruker D8-Venture diffractometer equipped with Cu (Cu/Kα radiation; λ =1.54178 Å) or Mo (Mo/Kα radiation; λ = 0.71073 Å) microfocus X-ray (IμS) sources, Photon CMOS detector and Oxford Cryosystems cooling device was used for data collection.

The frames were integrated with the Bruker SAINT software package using a narrow-frame algorithm. Data were corrected for absorption effects using the Multi-Scan method (SADABS). Obtained data were treated by XT-version 2014/5 and SHELXL-2014/7 software implemented in APEX3 v2016.5-0 (Bruker AXS) system.[S2]

Hydrogen atoms were mostly localized on a difference Fourier map, however to ensure uniformity of treatment of crystal, all hydrogen were recalculated into idealized positions (riding model) and assigned temperature factors $H_{iso}(H)$ = 1.2 U_{eq} (pivot atom) or of 1.5U_{eq} (methyl). H atoms in methyl and methylene and hydrogen atoms in aromatic rings were placed with C-H distances of 0.96, 0.97 and 0.93Å and 0.82 Å for O-H bonds.

$R_{int} = \sum | F_o^2 - F_{o,mean}^2 | / \sum F_o^2$, GOF = $[\sum(w(F_o^2 - F_c^2)^2)/(N_{diffrs} - N_{params})]^{½}$ for all data, $R(F) = \sum | |F_o| - |F_c| | / \sum |F_o|$ for observed data, $wR(F^2) = [\sum(w(F_o^2 - F_c^2)^2)/(\sum w(F_o^2)^2)]^{½}$ for all data.

Crystallographic data for structural analysis have been deposited with the Cambridge Crystallographic Data Centre, CCDC nos. 1955796-1955797. Copies of this information may be obtained free of charge from The Director, CCDC, 12 Union Road, Cambridge CB2 1EY, UK (fax: +44-1223-336033; e-mail: deposit@ccdc.cam.ac.uk or www: http://www.ccdc.cam.ac.uk).

Both crystals of **3 and 4** were of poor quality materials, which revealed weak diffraction patterns. Some of the positions of methylene, methyl or methoxy chains are disordered to the two or three positions with nearly equal occupancy. Disorders of these atoms are treated by standard methods.

Table S1. Crystal data and structure refinement for **3** (pz190509Zn1).

Identification code	pz190509Zn1
Empirical formula	$C_{58.75}H_{90.50}N_{24}O_{3.75}Zn$
Formula weight	1258.42
Temperature	150(2) K
Wavelength	0.71073 A
Crystal system, space group	Monoclinic, *C*2/c
Unit cell dimensions	a = 29.806(2) Å α = 90°
	b = 26.1290(16) Å β = 94.812(2)°
	c = 18.2989(11) Å γ = 90°

Volume	14201.0(15) Å^3
Z, Calculated density	8, 1.177 Mg/m^3
Absorption coefficient	0.405 mm^{-1}
F(000)	5368
Crystal size	0.646 x 0.432 x 0.424 mm
Theta range for data collection	2.234 to 26.000 deg.
Limiting indices	-36<=h<=36, -32<=k<=32, -22<=l<=22
Reflections collected / unique	203511 / 13927 [R(int) = 0.0960]
Completeness to theta = 25.242	99.5 %
Absorption correction	Semi-empirical from equivalents
Max. and min. transmission	0.8620 and 0.8095
Refinement method	Full-matrix least-squares on F^2
Data / restraints / parameters	13927 / 1048 / 906
Goodness-of-fit on F^2	1.061
Final R indices [I>2sigma(I)]	R_1 = 0.0673, wR_2 = 0.1883
R indices (all data)	R1 = 0.0863, wR2 = 0.1989
Extinction coefficient	n/a
Largest diff. peak and hole	1.551 and -0.817 e.A^{-3}

Table S2. Bond lengths [A] and angles [deg] for **3** (pz190509Zn1).

Zn(1)-N(5)	2.018(3)
Zn(1)-N(3)	2.025(3)
Zn(1)-N(7)	2.032(3)
Zn(1)-N(1)	2.033(3)
Zn(1)-O(1)	2.091(2)
N(1)-C(1)	1.365(4)
N(1)-C(4)	1.369(4)
N(2)-C(4)	1.324(4)
N(2)-C(5)	1.332(4)
N(3)-C(5)	1.363(4)
N(3)-C(8)	1.370(4)
N(4)-C(8)	1.328(4)
N(4)-C(9)	1.334(4)
N(5)-C(9)	1.374(4)
N(5)-C(12)	1.375(4)
N(6)-C(12)	1.329(4)
N(6)-C(13)	1.337(4)
N(7)-C(16)	1.362(4)
N(7)-C(13)	1.368(4)
N(8)-C(16)	1.325(4)
N(8)-C(1)	1.326(4)
N(9)-C(17)	1.324(4)
N(9)-C(2)	1.348(4)
N(10)-C(18)	1.327(4)
N(10)-C(3)	1.348(4)
N(11)-C(27)	1.333(5)
N(11)-C(6)	1.346(4)
N(12)-C(28)	1.330(5)
N(12)-C(7)	1.353(5)
N(13)-C(37)	1.328(5)
N(13)-C(10)	1.353(4)
N(14)-C(38)	1.333(5)
N(14)-C(11)	1.348(4)
N(15)-C(47)	1.316(4)
N(15)-C(14)	1.360(4)
N(16)-C(48)	1.333(4)
N(16)-C(15)	1.346(4)
N(17)-C(17)	1.395(4)
N(17)-C(19)	1.453(5)
N(17)-C(21)	1.479(5)
N(18)-C(18)	1.382(4)
N(18)-C(25)	1.460(5)
N(18)-C(23)	1.500(5)
N(19)-C(27)	1.384(5)
N(19)-C(29)	1.461(6)
N(19)-C(31)	1.469(6)
N(20)-C(28)	1.390(5)
N(20)-C(35)	1.472(8)
N(20)-C(35')	1.479(7)
N(20)-C(33)	1.484(7)
N(21)-C(37)	1.399(5)
N(21)-C(39)	1.476(6)
N(21)-C(41)	1.501(7)

N(22)-C(38)	1.386(5)
N(22)-C(43)	1.445(9)
N(22)-C(43')	1.472(7)
N(22)-C(45)	1.476(5)
N(23)-C(47)	1.397(4)
N(23)-C(49)	1.448(6)
N(23)-C(51)	1.483(6)
N(24)-C(48)	1.371(4)
N(24)-C(55)	1.465(5)
N(24)-C(53)	1.501(6)
C(1)-C(2)	1.448(4)
C(2)-C(3)	1.380(4)
C(3)-C(4)	1.460(4)
C(5)-C(6)	1.456(4)
C(6)-C(7)	1.363(5)
C(7)-C(8)	1.464(5)
C(9)-C(10)	1.451(5)
C(10)-C(11)	1.369(5)
C(11)-C(12)	1.449(4)
C(13)-C(14)	1.447(4)
C(14)-C(15)	1.377(4)
C(15)-C(16)	1.451(4)
C(17)-C(18)	1.466(5)
C(19)-C(20)	1.519(5)
C(21)-C(22)	1.494(7)
C(23)-C(24)	1.474(7)
C(25)-C(26)	1.482(7)
C(27)-C(28)	1.457(6)
C(29)-C(30')	1.512(10)
C(29)-C(30)	1.540(8)
C(31)-C(32)	1.520(8)
C(31)-C(32')	1.551(9)
C(33)-C(34)	1.481(9)
C(35)-C(36)	1.534(9)
C(35')-C(36')	1.537(8)
C(37)-C(38)	1.458(5)
C(39)-C(40)	1.520(7)
C(39)-C(40')	1.540(10)
C(41)-C(42)	1.525(6)
C(41)-C(42')	1.540(10)
C(43)-C(44)	1.524(9)
C(43')-C(44')	1.547(9)
C(45)-C(46)	1.537(9)
C(45)-C(46')	1.541(9)
C(47)-C(48)	1.468(5)
C(49)-C(50)	1.525(7)
C(51)-C(52)	1.530(7)
C(51)-C(52')	1.545(10)
C(53)-C(54')	1.531(7)
C(53)-C(54)	1.535(10)
C(55)-C(56)	1.527(8)
O(4S)-C(8S)	1.391(11)
O(4S)-C(8S)#1	1.391(11)
C(8S)-C(9S)	1.583(9)
C(9S)-C(9S)#1	1.530(9)

N(5)-Zn(1)-N(3)	87.79(11)

N(5)-Zn(1)-N(7)	86.57(10)
N(3)-Zn(1)-N(7)	154.25(10)
N(5)-Zn(1)-N(1)	154.43(11)
N(3)-Zn(1)-N(1)	86.86(10)
N(7)-Zn(1)-N(1)	87.48(10)
N(5)-Zn(1)-O(1)	101.61(10)
N(3)-Zn(1)-O(1)	101.69(10)
N(7)-Zn(1)-O(1)	104.06(10)
N(1)-Zn(1)-O(1)	103.96(10)
C(1)-N(1)-C(4)	108.8(2)
C(1)-N(1)-Zn(1)	125.2(2)
C(4)-N(1)-Zn(1)	125.7(2)
C(4)-N(2)-C(5)	123.4(3)
C(5)-N(3)-C(8)	109.3(3)
C(5)-N(3)-Zn(1)	125.1(2)
C(8)-N(3)-Zn(1)	124.8(2)
C(8)-N(4)-C(9)	123.8(3)
C(9)-N(5)-C(12)	108.8(3)
C(9)-N(5)-Zn(1)	125.2(2)
C(12)-N(5)-Zn(1)	125.2(2)
C(12)-N(6)-C(13)	122.9(3)
C(16)-N(7)-C(13)	108.5(3)
C(16)-N(7)-Zn(1)	124.9(2)
C(13)-N(7)-Zn(1)	126.3(2)
C(16)-N(8)-C(1)	123.3(3)
C(17)-N(9)-C(2)	114.7(3)
C(18)-N(10)-C(3)	114.8(3)
C(27)-N(11)-C(6)	114.9(3)
C(28)-N(12)-C(7)	114.9(3)
C(37)-N(13)-C(10)	114.7(3)
C(38)-N(14)-C(11)	114.8(3)
C(47)-N(15)-C(14)	114.8(3)
C(48)-N(16)-C(15)	114.6(3)
C(17)-N(17)-C(19)	116.1(3)
C(17)-N(17)-C(21)	114.7(3)
C(19)-N(17)-C(21)	115.3(3)
C(18)-N(18)-C(25)	117.2(3)
C(18)-N(18)-C(23)	117.1(3)
C(25)-N(18)-C(23)	115.6(3)
C(27)-N(19)-C(29)	118.6(4)
C(27)-N(19)-C(31)	118.4(3)
C(29)-N(19)-C(31)	115.9(4)
C(28)-N(20)-C(35)	118.7(7)
C(28)-N(20)-C(35')	114.9(5)
C(28)-N(20)-C(33)	116.3(4)
C(35)-N(20)-C(33)	101.9(6)
C(35')-N(20)-C(33)	122.1(6)
C(37)-N(21)-C(39)	116.6(4)
C(37)-N(21)-C(41)	114.2(4)
C(39)-N(21)-C(41)	115.5(4)
C(38)-N(22)-C(43)	113.8(6)
C(38)-N(22)-C(43')	118.4(4)
C(38)-N(22)-C(45)	121.2(4)
C(43)-N(22)-C(45)	122.9(7)
C(43')-N(22)-C(45)	109.6(6)
C(47)-N(23)-C(49)	116.4(3)
C(47)-N(23)-C(51)	112.9(3)

C(49)-N(23)-C(51)	112.2(4)
C(48)-N(24)-C(55)	116.9(3)
C(48)-N(24)-C(53)	118.1(3)
C(55)-N(24)-C(53)	111.1(3)
N(8)-C(1)-N(1)	128.1(3)
N(8)-C(1)-C(2)	122.8(3)
N(1)-C(1)-C(2)	109.0(3)
N(9)-C(2)-C(3)	123.6(3)
N(9)-C(2)-C(1)	129.3(3)
C(3)-C(2)-C(1)	106.9(3)
N(10)-C(3)-C(2)	122.9(3)
N(10)-C(3)-C(4)	130.3(3)
C(2)-C(3)-C(4)	106.8(3)
N(2)-C(4)-N(1)	127.5(3)
N(2)-C(4)-C(3)	124.1(3)
N(1)-C(4)-C(3)	108.4(3)
N(2)-C(5)-N(3)	128.1(3)
N(2)-C(5)-C(6)	123.4(3)
N(3)-C(5)-C(6)	108.5(3)
N(11)-C(6)-C(7)	123.7(3)
N(11)-C(6)-C(5)	129.2(3)
C(7)-C(6)-C(5)	107.0(3)
N(12)-C(7)-C(6)	122.8(3)
N(12)-C(7)-C(8)	129.4(3)
C(6)-C(7)-C(8)	107.5(3)
N(4)-C(8)-N(3)	127.9(3)
N(4)-C(8)-C(7)	124.5(3)
N(3)-C(8)-C(7)	107.6(3)
N(4)-C(9)-N(5)	127.4(3)
N(4)-C(9)-C(10)	124.4(3)
N(5)-C(9)-C(10)	108.2(3)
N(13)-C(10)-C(11)	122.6(3)
N(13)-C(10)-C(9)	129.9(3)
C(11)-C(10)-C(9)	107.4(3)
N(14)-C(11)-C(10)	124.2(3)
N(14)-C(11)-C(12)	128.5(3)
C(10)-C(11)-C(12)	107.3(3)
N(6)-C(12)-N(5)	128.2(3)
N(6)-C(12)-C(11)	123.4(3)
N(5)-C(12)-C(11)	108.3(3)
N(6)-C(13)-N(7)	126.9(3)
N(6)-C(13)-C(14)	124.2(3)
N(7)-C(13)-C(14)	108.9(3)
N(15)-C(14)-C(15)	122.0(3)
N(15)-C(14)-C(13)	130.8(3)
C(15)-C(14)-C(13)	106.9(3)
N(16)-C(15)-C(14)	124.7(3)
N(16)-C(15)-C(16)	128.6(3)
C(14)-C(15)-C(16)	106.7(3)
N(8)-C(16)-N(7)	128.8(3)
N(8)-C(16)-C(15)	122.2(3)
N(7)-C(16)-C(15)	109.0(3)
N(9)-C(17)-N(17)	118.1(3)
N(9)-C(17)-C(18)	121.3(3)
N(17)-C(17)-C(18)	120.6(3)
N(10)-C(18)-N(18)	118.3(3)
N(10)-C(18)-C(17)	121.7(3)

N(18)-C(18)-C(17)	120.0(3)
N(17)-C(19)-C(20)	111.7(3)
N(17)-C(21)-C(22)	114.0(4)
C(24)-C(23)-N(18)	114.0(5)
N(18)-C(25)-C(26)	111.7(4)
N(11)-C(27)-N(19)	117.4(4)
N(11)-C(27)-C(28)	121.1(3)
N(19)-C(27)-C(28)	121.5(3)
N(12)-C(28)-N(20)	116.9(4)
N(12)-C(28)-C(27)	121.7(3)
N(20)-C(28)-C(27)	121.4(3)
N(19)-C(29)-C(30')	110.7(11)
N(19)-C(29)-C(30)	113.6(5)
N(19)-C(31)-C(32)	112.9(7)
N(19)-C(31)-C(32')	108.9(9)
C(34)-C(33)-N(20)	113.0(5)
N(20)-C(35)-C(36)	105.3(9)
N(20)-C(35')-C(36')	117.9(7)
N(13)-C(37)-N(21)	117.5(3)
N(13)-C(37)-C(38)	122.5(3)
N(21)-C(37)-C(38)	119.9(3)
N(14)-C(38)-N(22)	116.6(3)
N(14)-C(38)-C(37)	120.9(3)
N(22)-C(38)-C(37)	122.5(3)
N(21)-C(39)-C(40)	110.1(4)
N(21)-C(39)-C(40')	139(4)
N(21)-C(41)-C(42)	113.9(4)
N(21)-C(41)-C(42')	99.4(6)
N(22)-C(43)-C(44)	116.1(14)
N(22)-C(43')-C(44')	106.1(10)
N(22)-C(45)-C(46)	108.8(7)
N(22)-C(45)-C(46')	116.3(7)
N(15)-C(47)-N(23)	118.3(3)
N(15)-C(47)-C(48)	122.9(3)
N(23)-C(47)-C(48)	118.8(3)
N(16)-C(48)-N(24)	117.9(3)
N(16)-C(48)-C(47)	120.6(3)
N(24)-C(48)-C(47)	121.5(3)
N(23)-C(49)-C(50)	110.0(4)
N(23)-C(51)-C(52)	113.1(5)
N(23)-C(51)-C(52')	131(3)
N(24)-C(53)-C(54')	109.8(6)
N(24)-C(53)-C(54)	119.6(14)
N(24)-C(55)-C(56)	109.9(4)
C(2S)-C(1S)-C(7S)	115.8(15)
C(6S)-C(1S)-C(7S)	124.0(15)
C(8S)-O(4S)-C(8S)#1	113.0(11)
O(4S)-C(8S)-C(9S)	109.1(8)
C(9S)#1-C(9S)-C(8S)	104.4(4)

Symmetry transformations used to generate equivalent atoms:
#1 -x+3,y,-z+1/2

Table S3. Crystal data and structure refinement for **4** (pz190507Zn1).

Identification code	pz190507Zn1
Empirical formula	$C_{72}H_{118.50}N_{24}O_{19.25}Zn$
Formula weight	1693.77
Temperature	150(2) K
Wavelength	0.71073 Å
Crystal system, space group	Triclinic, *P*-1
Unit cell dimensions	a = 15.5889(6) Å α = 86.233(2)°.
	b = 15.9560(7) Å β = 71.563(2)°.
	c = 19.7600(8) Å γ = 68.105(2) °.
Volume	4318.8(3) $Å^3$
Z, Calculated density	2, 1.302 Mg/m^3
Absorption coefficient	0.364 mm^{-1}
F(000)	1805
Crystal size	1.036 x 0.418 x 0.264 mm
Theta range for data collection	2.371 to 26.000 deg.
Limiting indices	-19<=h<=19, -19<=k<=19, -24<=l<=24
Reflections collected / unique	117332 / 16921 [R(int) = 0.0847]
Completeness to theta = 25.242	99.7 %
Absorption correction	Semi-empirical from equivalents
Max. and min. transmission	0.8620 and 0.7832
Refinement method	Full-matrix least-squares on F^2
Data / restraints / parameters	16921 / 1344 / 1166
Goodness-of-fit on F^2	1.103
Final R indices [I>2sigma(I)]	R1 = 0.0709, wR2 = 0.1960
R indices (all data)	R_1 = 0.1025, wR_2 = 0.2178
Extinction coefficient	n/a
Largest diff. peak and hole	1.120 and -0.822 $eÅ^{-3}$

Table S4. Bond lengths [A] and angles [deg] for **4** (pz190507Zn1).

Zn(1)-N(3)	2.011(2)
Zn(1)-N(5)	2.023(3)
Zn(1)-N(1)	2.029(2)
Zn(1)-N(7)	2.031(2)
Zn(1)-O(1S)	2.086(3)
O(1S)-H(1)	0.899(10)
O(1S)-H(2)	0.902(10)
N(1)-C(1)	1.369(4)
N(1)-C(4)	1.374(4)
N(2)-C(4)	1.327(4)
N(2)-C(5)	1.336(4)
N(3)-C(5)	1.370(4)
N(3)-C(8)	1.373(4)
N(4)-C(8)	1.322(4)
N(4)-C(9)	1.331(4)
N(5)-C(9)	1.372(4)
N(5)-C(12)	1.373(4)
N(6)-C(12)	1.325(4)

N(6)-C(13)	1.335(4)
N(7)-C(16)	1.368(4)
N(7)-C(13)	1.369(4)
N(8)-C(16)	1.322(4)
N(8)-C(1)	1.331(4)
N(9)-C(31)	1.332(4)
N(9)-C(6)	1.341(4)
N(10)-C(32)	1.317(4)
N(10)-C(7)	1.351(4)
N(11)-C(45)	1.321(5)
N(11)-C(10)	1.359(4)
N(12)-C(46)	1.334(4)
N(12)-C(11)	1.339(4)
N(13)-C(59)	1.327(4)
N(13)-C(14)	1.358(4)
N(14)-C(60)	1.325(4)
N(14)-C(15)	1.359(4)
N(15)-C(17)	1.321(4)
N(15)-C(2)	1.347(4)
N(16)-C(18)	1.329(4)
N(16)-C(3)	1.347(4)
N(17)-C(31)	1.386(4)
N(17)-C(36)	1.453(9)
N(17)-C(36')	1.461(9)
N(17)-C(33)	1.501(6)
N(17)-C(36'')	1.503(9)
N(18)-C(32)	1.381(4)
N(18)-C(39)	1.459(5)
N(18)-C(42)	1.471(5)
N(19)-C(45)	1.390(4)
N(19)-C(50)	1.459(6)
N(19)-C(47)	1.464(6)
N(20)-C(46)	1.385(5)
N(20)-C(53)	1.448(6)
N(20)-C(56)	1.474(6)
N(21)-C(59)	1.390(4)
N(21)-C(61)	1.462(5)
N(21)-C(64)	1.468(5)
N(22)-C(60)	1.377(4)
N(22)-C(67)	1.465(4)
N(22)-C(70)	1.479(4)
N(23)-C(17)	1.393(4)
N(23)-C(22)	1.453(5)
N(23)-C(19)	1.467(4)
N(24)-C(18)	1.392(4)
N(24)-C(28)	1.473(4)
N(24)-C(25)	1.478(5)
C(1)-C(2)	1.439(4)
C(2)-C(3)	1.375(4)
C(3)-C(4)	1.462(4)
C(5)-C(6)	1.458(4)
C(6)-C(7)	1.377(4)
C(7)-C(8)	1.447(4)
C(9)-C(10)	1.451(4)
C(10)-C(11)	1.376(5)
C(11)-C(12)	1.457(4)
C(13)-C(14)	1.453(4)

C(14)-C(15)	1.371(4)
C(15)-C(16)	1.451(4)
C(17)-C(18)	1.461(4)
C(19)-C(20)	1.501(5)
C(20)-O(1')	1.314(6)
C(20)-O(1)	1.350(6)
O(1)-C(21)	1.409(7)
O(1')-C(21')	1.448(10)
C(22)-C(23)	1.506(7)
C(23)-O(2)	1.404(6)
O(2)-C(24')	1.428(14)
O(2)-C(24)	1.464(15)
C(25)-C(26)	1.505(5)
C(26)-O(3)	1.386(6)
O(3)-C(27')	1.430(12)
O(3)-C(27)	1.473(12)
C(28)-C(29)	1.479(7)
C(29)-O(4)	1.427(5)
O(4)-C(30)	1.425(7)
C(31)-C(32)	1.463(5)
C(33)-C(34)	1.536(9)
C(34)-O(5)	1.433(9)
O(5)-C(35')	1.431(9)
O(5)-C(35)	1.438(9)
C(39)-C(40)	1.524(7)
C(40)-O(8)	1.378(6)
O(8)-C(41)	1.438(8)
C(42)-C(43)	1.466(7)
C(43)-O(7')	1.404(9)
C(43)-O(7)	1.457(7)
O(7)-C(44)	1.433(8)
O(7')-C(44')	1.436(10)
C(45)-C(46)	1.463(5)
C(47)-C(48)	1.473(8)
C(48)-O(9)	1.423(6)
O(9)-C(49)	1.403(8)
O(9)-C(49')	1.441(8)
C(50)-C(51)	1.458(12)
C(50)-C(51')	1.517(19)
C(51)-O(10)	1.416(8)
O(10)-C(52)	1.425(8)
C(51')-O(10')	1.418(9)
O(10')-C(52')	1.418(9)
C(53)-C(54')	1.525(10)
C(53)-C(54)	1.531(8)
C(54)-O(11)	1.448(8)
O(11)-C(55)	1.415(8)
C(54')-O(11')	1.436(10)
O(11')-C(55')	1.452(10)
C(56)-C(57)	1.398(14)
C(56)-C(57')	1.568(14)
C(57)-O(12)	1.388(7)
O(12)-C(58)	1.389(9)
C(57')-O(12')	1.466(9)
O(12')-C(58')	1.426(9)
C(59)-C(60)	1.466(4)
C(61)-C(62)	1.517(6)

C(62)-O(13)	1.372(7)
O(13)-C(63)	1.428(6)
C(64)-C(65)	1.447(7)
C(65)-O(14')	1.363(6)
C(65)-O(14)	1.367(6)
O(14)-C(66)	1.416(8)
O(14')-C(66')	1.427(9)
C(67)-C(68)	1.493(5)
C(68)-O(15)	1.410(5)
O(15)-C(69)	1.419(6)
C(70)-C(71)	1.493(5)
C(71)-O(16')	1.396(5)
C(71)-O(16)	1.402(9)
O(16)-C(72)	1.427(10)
O(16')-C(72')	1.427(6)
O(6)-C(38)	1.401(10)
O(6)-C(37)	1.441(9)
C(36)-C(37)	1.549(10)
O(6')-C(37')	1.427(9)
O(6')-C(38')	1.444(10)
C(36')-C(37')	1.529(10)
O(6")-C(38")	1.430(10)
O(6")-C(37")	1.449(9)
C(36")-C(37")	1.544(9)

N(3)-Zn(1)-N(5)	88.69(10)
N(3)-Zn(1)-N(1)	86.56(10)
N(5)-Zn(1)-N(1)	155.92(12)
N(3)-Zn(1)-N(7)	154.54(11)
N(5)-Zn(1)-N(7)	86.47(10)
N(1)-Zn(1)-N(7)	87.74(10)
N(3)-Zn(1)-O(1S)	99.81(10)
N(5)-Zn(1)-O(1S)	104.48(10)
N(1)-Zn(1)-O(1S)	99.59(10)
N(7)-Zn(1)-O(1S)	105.61(10)
C(1)-N(1)-C(4)	108.5(2)
C(1)-N(1)-Zn(1)	124.2(2)
C(4)-N(1)-Zn(1)	125.71(19)
C(4)-N(2)-C(5)	123.3(3)
C(5)-N(3)-C(8)	109.0(2)
C(5)-N(3)-Zn(1)	126.58(19)
C(8)-N(3)-Zn(1)	124.2(2)
C(8)-N(4)-C(9)	124.0(3)
C(9)-N(5)-C(12)	108.6(3)
C(9)-N(5)-Zn(1)	124.7(2)
C(12)-N(5)-Zn(1)	126.6(2)
C(12)-N(6)-C(13)	123.1(3)
C(16)-N(7)-C(13)	108.5(2)
C(16)-N(7)-Zn(1)	124.1(2)
C(13)-N(7)-Zn(1)	126.9(2)
C(16)-N(8)-C(1)	124.0(2)
C(31)-N(9)-C(6)	114.2(3)
C(32)-N(10)-C(7)	114.5(3)
C(45)-N(11)-C(10)	114.7(3)
C(46)-N(12)-C(11)	115.0(3)
C(59)-N(13)-C(14)	113.9(3)
C(60)-N(14)-C(15)	113.7(3)

C(17)-N(15)-C(2)	115.0(3)
C(18)-N(16)-C(3)	114.7(3)
C(31)-N(17)-C(36)	119.9(9)
C(31)-N(17)-C(36')	115.8(8)
C(31)-N(17)-C(33)	114.8(4)
C(36)-N(17)-C(33)	108.3(8)
C(36')-N(17)-C(33)	115.6(9)
C(31)-N(17)-C(36'')	113.3(7)
C(33)-N(17)-C(36'')	125.8(8)
C(32)-N(18)-C(39)	119.0(3)
C(32)-N(18)-C(42)	117.0(3)
C(39)-N(18)-C(42)	115.3(3)
C(45)-N(19)-C(50)	117.0(3)
C(45)-N(19)-C(47)	117.0(3)
C(50)-N(19)-C(47)	115.3(3)
C(46)-N(20)-C(53)	117.7(3)
C(46)-N(20)-C(56)	119.4(4)
C(53)-N(20)-C(56)	117.2(4)
C(59)-N(21)-C(61)	117.5(3)
C(59)-N(21)-C(64)	115.6(3)
C(61)-N(21)-C(64)	116.5(3)
C(60)-N(22)-C(67)	117.9(3)
C(60)-N(22)-C(70)	119.1(3)
C(67)-N(22)-C(70)	116.6(3)
C(17)-N(23)-C(22)	114.8(3)
C(17)-N(23)-C(19)	115.1(3)
C(22)-N(23)-C(19)	115.2(3)
C(18)-N(24)-C(28)	114.8(3)
C(18)-N(24)-C(25)	116.2(3)
C(28)-N(24)-C(25)	113.9(3)
N(8)-C(1)-N(1)	127.6(3)
N(8)-C(1)-C(2)	123.5(3)
N(1)-C(1)-C(2)	108.9(2)
N(15)-C(2)-C(3)	123.4(3)
N(15)-C(2)-C(1)	128.7(3)
C(3)-C(2)-C(1)	107.7(2)
N(16)-C(3)-C(2)	122.7(3)
N(16)-C(3)-C(4)	130.7(3)
C(2)-C(3)-C(4)	106.4(3)
N(2)-C(4)-N(1)	126.9(3)
N(2)-C(4)-C(3)	124.7(3)
N(1)-C(4)-C(3)	108.4(2)
N(2)-C(5)-N(3)	127.5(3)
N(2)-C(5)-C(6)	124.0(3)
N(3)-C(5)-C(6)	108.5(3)
N(9)-C(6)-C(7)	123.0(3)
N(9)-C(6)-C(5)	129.9(3)
C(7)-C(6)-C(5)	106.6(3)
N(10)-C(7)-C(6)	123.5(3)
N(10)-C(7)-C(8)	128.8(3)
C(6)-C(7)-C(8)	107.6(3)
N(4)-C(8)-N(3)	128.6(3)
N(4)-C(8)-C(7)	123.1(3)
N(3)-C(8)-C(7)	108.3(3)
N(4)-C(9)-N(5)	127.4(3)
N(4)-C(9)-C(10)	123.9(3)
N(5)-C(9)-C(10)	108.5(3)

N(11)-C(10)-C(11)	122.6(3)
N(11)-C(10)-C(9)	129.5(3)
C(11)-C(10)-C(9)	107.5(3)
N(12)-C(11)-C(10)	123.7(3)
N(12)-C(11)-C(12)	129.6(3)
C(10)-C(11)-C(12)	106.6(3)
N(6)-C(12)-N(5)	128.1(3)
N(6)-C(12)-C(11)	123.2(3)
N(5)-C(12)-C(11)	108.7(3)
N(6)-C(13)-N(7)	127.0(3)
N(6)-C(13)-C(14)	124.1(3)
N(7)-C(13)-C(14)	108.9(2)
N(13)-C(14)-C(15)	122.8(3)
N(13)-C(14)-C(13)	129.9(3)
C(15)-C(14)-C(13)	106.7(3)
N(14)-C(15)-C(14)	124.0(3)
N(14)-C(15)-C(16)	128.7(3)
C(14)-C(15)-C(16)	107.3(3)
N(8)-C(16)-N(7)	128.3(3)
N(8)-C(16)-C(15)	123.1(3)
N(7)-C(16)-C(15)	108.6(2)
N(15)-C(17)-N(23)	118.1(3)
N(15)-C(17)-C(18)	121.0(3)
N(23)-C(17)-C(18)	120.9(3)
N(16)-C(18)-N(24)	118.3(3)
N(16)-C(18)-C(17)	121.6(3)
N(24)-C(18)-C(17)	120.1(3)
N(23)-C(19)-C(20)	112.9(3)
O(1')-C(20)-C(19)	119.1(5)
O(1)-C(20)-C(19)	106.0(4)
C(20)-O(1)-C(21)	111.7(6)
C(20)-O(1')-C(21')	113.7(7)
N(23)-C(22)-C(23)	115.4(3)
O(2)-C(23)-C(22)	107.6(4)
C(23)-O(2)-C(24')	102.8(7)
C(23)-O(2)-C(24)	122.4(7)
N(24)-C(25)-C(26)	114.8(3)
O(3)-C(26)-C(25)	111.9(4)
C(26)-O(3)-C(27')	120.4(6)
C(26)-O(3)-C(27)	105.9(6)
N(24)-C(28)-C(29)	111.4(4)
O(4)-C(29)-C(28)	114.3(4)
C(30)-O(4)-C(29)	112.7(4)
N(9)-C(31)-N(17)	117.7(3)
N(9)-C(31)-C(32)	121.7(3)
N(17)-C(31)-C(32)	120.6(3)
N(10)-C(32)-N(18)	117.6(3)
N(10)-C(32)-C(31)	121.1(3)
N(18)-C(32)-C(31)	121.2(3)
N(17)-C(33)-C(34)	112.3(4)
O(5)-C(34)-C(33)	107.7(5)
C(35')-O(5)-C(34)	106.4(9)
C(34)-O(5)-C(35)	122.8(9)
N(18)-C(39)-C(40)	111.0(3)
O(8)-C(40)-C(39)	110.4(4)
C(40)-O(8)-C(41)	111.6(5)
C(43)-C(42)-N(18)	112.3(4)

O(7')-C(43)-C(42)	124.9(10)
O(7)-C(43)-C(42)	102.5(5)
C(44)-O(7)-C(43)	108.7(7)
C(43)-O(7')-C(44')	119.6(19)
N(11)-C(45)-N(19)	118.1(3)
N(11)-C(45)-C(46)	122.0(3)
N(19)-C(45)-C(46)	119.9(3)
N(12)-C(46)-N(20)	117.2(3)
N(12)-C(46)-C(45)	120.7(3)
N(20)-C(46)-C(45)	122.0(3)
N(19)-C(47)-C(48)	112.3(4)
O(9)-C(48)-C(47)	108.5(4)
C(49)-O(9)-C(48)	105.3(7)
C(48)-O(9)-C(49')	114.6(7)
C(51)-C(50)-N(19)	114.0(6)
N(19)-C(50)-C(51')	111.9(8)
O(10)-C(51)-C(50)	103.2(7)
C(51)-O(10)-C(52)	116.1(9)
O(10')-C(51')-C(50)	112.5(13)
C(51')-O(10')-C(52')	117.9(14)
N(20)-C(53)-C(54')	122.6(17)
N(20)-C(53)-C(54)	109.0(6)
O(11)-C(54)-C(53)	103.3(7)
C(55)-O(11)-C(54)	109.3(8)
O(11')-C(54')-C(53)	88.2(13)
C(54')-O(11')-C(55')	118(2)
C(57)-C(56)-N(20)	122.1(5)
N(20)-C(56)-C(57')	106.7(6)
O(12)-C(57)-C(56)	115.4(9)
C(57)-O(12)-C(58)	125.9(11)
O(12')-C(57')-C(56)	100.4(8)
C(58')-O(12')-C(57')	105.0(10)
N(13)-C(59)-N(21)	118.5(3)
N(13)-C(59)-C(60)	122.0(3)
N(21)-C(59)-C(60)	119.4(3)
N(14)-C(60)-N(22)	118.7(3)
N(14)-C(60)-C(59)	121.1(3)
N(22)-C(60)-C(59)	120.1(3)
N(21)-C(61)-C(62)	111.3(3)
O(13)-C(62)-C(61)	111.4(4)
C(62)-O(13)-C(63)	111.9(5)
C(65)-C(64)-N(21)	115.6(3)
O(14')-C(65)-C(64)	130.0(6)
O(14)-C(65)-C(64)	111.2(5)
C(65)-O(14)-C(66)	113.0(8)
C(65)-O(14')-C(66')	115.1(10)
N(22)-C(67)-C(68)	111.1(3)
O(15)-C(68)-C(67)	108.5(3)
C(68)-O(15)-C(69)	111.7(4)
N(22)-C(70)-C(71)	114.5(4)
O(16')-C(71)-C(70)	110.1(4)
O(16)-C(71)-C(70)	113.7(7)
C(71)-O(16)-C(72)	112(2)
C(71)-O(16')-C(72')	110.1(5)
C(38)-O(6)-C(37)	120.5(17)
N(17)-C(36)-C(37)	101.5(12)
O(6)-C(37)-C(36)	119.7(16)

C(37')-O(6')-C(38')	106.1(13)
N(17)-C(36')-C(37')	108.2(13)
O(6')-C(37')-C(36')	105.7(15)
C(38")-O(6")-C(37")	121.9(16)
N(17)-C(36")-C(37")	123.6(11)
O(6")-C(37")-C(36")	112.4(12)

References

1. Demuth, J.; Kucera, R.; Kopecky, K.; Havlínová, Z.; Libra, A.; Novakova, V.; Miletin, M.; Zimcik, P., Efficient Synthesis of a Wide-Range Absorbing Azaphthalocyanine Dark Quencher and Its Application to Dual-Labeled Oligonucleotide Probes for Quantitative Real-Time Polymerase Chain Reactions. *Chemistry – A European Journal* **2018,** 24, (38), 9658-9666.
2. Petrik, P.; Zimcik, P.; Kopecky, K.; Musil, Z.; Miletin, M.; Loukotova, V., Protonation and deprotonation of nitrogens in tetrapyrazinoporphyrazine macrocycles. *Journal of Porphyrins and Phthalocyanines* **2007,** 11, 487-495.
3. Kopecky, K.; Novakova, V.; Miletin, M.; Kucera, R.; Zimcik, P., Synthesis of new azaphthalocyanine dark quencher and evaluation of its quenching efficiency with different fluorophores. *Tetrahedron* **2011,** 67, (33), 5956-5963.
4. Inaba, Y.; Kobuke, Y., Synthesis of a complementary dimer from mono(imidazolyl)-substituted cobalt(II) porphyrin as a new artificial T-form hemoglobin. *Tetrahedron* **2004,** 60, (13), 3097-3107.
5. García-Iglesias, M.; Peuntinger, K.; Kahnt, A.; Krausmann, J.; Vázquez, P.; González-Rodríguez, D.; Guldi, D. M.; Torres, T., Supramolecular Assembly of Multicomponent Photoactive Systems via Cooperatively Coupled Equilibria. *Journal of the American Chemical Society* **2013,** 135, (51), 19311-19318.
6. Libra, A.; Fernetti, C.; Lorusso, V.; Visigalli, M.; Anelli, P. L.; Staud, F.; Tiribelli, C.; Pascolo, L., Molecular determinants in the transport of a bile acid-derived diagnostic agent in tumoral and nontumoral cell lines of human liver. *Journal of Pharmacology and Experimental Therapeutics* **2006,** 319, (2), 809-817.